Evaluation of Gravity Field Models:

EIGEN-6C4 and GOCO03S combined with EGM08 using GNSS-Levelling

A thesis submitted to Adama Science and Technology University in partial fulfilment of the requirement for Master of Science in Geodesy and Geomatics Engineering

Zerihun Geremew Gebresenbet

Adama, Ethiopia

May, 2017

Declaration

I confirm that the work in this thesis is my own and has not been presented for academic award in any university or institution and will not be presented in any other university or institution for any academic award.

Zerihun Geremew Gebresenbet ______________________ ____________________.

Signature Date

I confirm that, to the best of my knowledge, the research was carried and the thesis was prepared under my direct supervision.

Dr. Tulu Besha Bedada _________________ ____________________.

Supervisor Signature Date

Approval

Adama Science and Technology University

School of Civil Engineering and Architecture

Geomatics Engineering Program

This undersigned hear by certify that they have read and recommend to the Adama Science and Technology University, school of civil engineering and architecture for acceptance a thesis entitled "**Evaluation of Gravity Field Models: EIGEN-6C4 and GOCO03S combined with EGM08 using GNSS-Levelling**" compiled by Zerihun Geremew Gebresenbet in the partial fulfilment of the requirement for the degree of Master of Science in Geodesy and Geomatics Engineering.

1.	Dr. Tulu Besha Bedada	______________	______________.
	Supervisor	signature	date
2.	______________________	______________	______________.
	External examiner	signature	date
3.	______________________	______________	______________.
	Internal examiner	signature	date
4.	______________________	______________	______________.
	Chairman	signature	date
5.	______________________	______________	______________.
	Program chair	signature	date
6.	______________________	______________	______________.
	School dean	signature	date

Abstract

This study has evaluated the accuracy of tow high resolution geopotential models. The objective of the study is to evaluate the accuracy of these global geopotential models such as EIGEN-6C4, and GOCO03S combined with the 2008 Earth Gravity Model (EGM08) using an independent Global Navigation Satellite System (GNSS) and levelling data. GOCO03S and EGM08 are combined by using Butterworth filter to synthesis a combined model that can recover long wavelengths from Gravity for steady-state Ocean Circulation Explorer (GOCE) satellite. GOCO03S is truncated to spherical harmonics up to degree and order of 240. The EIGEN-6C4 combines EGM08 and new gravitational information from GOCE satellite when compared to GOCO03S. Space domain spherical harmonic analysis was used to determine geopotential heights and geoid heights from GOCO03S plus EGM08, and EIGEN-6C4 at five GNSS-levelling bench marks across 10.742 km baseline between Addis Ababa and Legedadi – levelled heights are connected to the Blue Nile bench marks. GNSS data was initially processed by GAMIT/GLOBK, AUSPOS service, RTX (Real Time eXtended) service and LGO (Leica Geo Office) with a tie to ITRF08 reference frame; accuracy was assessed and later geodetic coordinates (longitude, latitude, ellipsoidal height) from GAMIT/GLOBK were used for the computation of geopotential heights and geoid heights at GNSS-levelling bench marks.

The accuracy of the geopotential heights computed from the EIGEN-6C4 geopotential model was evaluated by comparing it with the one derived from GOCO03S combined with EGM08 and precise levelled heights. The geoid heights computed from the two geopotential models are also compared with geoid heights derived from GNSS-levelling data.

The EIGEN-6C4 model is in a good agreement with a standard deviation of 0.002m and 0.111m relative to GOCO03S plus EGM08 and levelling, respectively. Moreover, the residual between levelled heights and orthometric heights computed from GOCO03S and EGM08 has standard deviation of 0.110m. Besides, the residual between the gravimetric geoid heights and geoid heights derived from GNSS-levelling has a mean of (0.111m for EIGEN-6C4 and 0.073m for GOCO03S plus EGM08) and standard deviation of (0.110m for EIGEN-6C4 and 0.109m for GOCO03S plus EGM08). The absolute height separation between the levelling datum and the geoid is 0.082m and 0.044m for EIGEN-6C4, and GOCO03S plus EGM08 respectively.

The results of the study showed that the combined geopotential model best simulates to the GNSS-levelling data compared to EIGEN-6C4 model. The discrepancy of -0.038m between the EIGEN-6C4 and GOCO03S and EGM08 models may arise from the computational methods employed in the synthesisation of Stoke's cosine and sine coefficients.

Key words: ***EIGEN-6C4, GOCO03S, EGM08, GNSS-Levelling***

Acknowledgment

First of all my thanks and honour goes to the '**Almighty God'**.

For most my profound gratitude with appreciation goes to my supervisor **Dr.Tulu Besha Bedada**, Assistance professor of Geodesy head, Earth observation division, Entoto Observatory and Research center (EORC), Addis Ababa, Ethiopia; for his generous treatment, complete guidance and sharing me knowledge from his well-grounded Physical Geodesy throughout the Project. His continuous strong advice and support make this project tangible.

Information Network Security Agency **(INSA)** has a great contribution in providing me personnel, Leica GNSS receivers and logistics; without this support this study would not have appeared. On behalf of INSA my special appreciation goes to **Colonel Tazer G/Egziabiher**, vice director of INSA and Geospatial data security directorate director for his giving me moral and support to carry out this project.

Many thanks go to **Getu Engda** and **Genanaw Alemu** from Geospatial data acquisition and processing team for their continuous support from proposal evaluation and approval to logistics preparation by providing constructive comments and giving me moral towards the accomplishment of the project.

I would like to tanks my workmates GNSS data observation crews: **Yonas Teklu** and **Yusuf Mohammed;** levelling crews: **Tofik Ali**, **Mohammednur Abdela** and **Zewudu Hailu** helping me during GNSS data observation and differential levelling resisting the hardship.

My special thanks also goes to my classmate **Jifara Dabessa** for his giving me level instrument with its accessories. I would also like to thank my classmate **Kindu Temesgen** and **Eshetu Nega** ,Ph.D. student in Geodesy at EORC for their contribution in GNSS data processing by GAMIT/GLOBKG.

Finally I am grateful to my wife **Fikirteyohannis Araya** and others not mentioned here giving me moral support during my study.

Contents

Table of contents

List of Tables

List of Figures

List of Acronyms

BS	Back Sight
BM	Bench mark
CCDG	Country Club Developers Gate
CHAMP	Challenging Mini-Satellite Payload
DEM	Digital Elevation Model
DGPS	Differential Global Positioning System
DOD	Department of Defence
DOP	Dilution of Precision
DOY	Day Of Year
DTU	Denmark University of Technology
EGM08	Earth Gravitational Model 2008
EGM96	Earth Gravitational Model 1996
EGM	Earth Gravitational Model
EIGEN	European Improved Gravity model of the Earth by New techniques
EMA	Ethiopian Mapping Agency
EORC	Entoto Observatory and Research Center
ESA	European Space Agency
EU	European Union
FGCS	Federal Geodetic Control Subcommittee
FS	Fore Sight
GCP	Ground Control Point
GDOP	Geometric Dilution of Precision
GFZ	Geo Forschungs Zentrum
GLONASS	Global Navigation Satellite System
GNSS	Global Navigation Satellite System
GOCE	Gravity field and steady-state Ocean Circulation Explorer
GOCO03S	Third generation GRACE and GOCE combined solution
GOCO	Gravity Observation Combination
GPS	Global Positioning System
GRACE	Gravity Recovery and Climate Experiment
GRGS	Groupe Recherches Geodesie Spatiale
ICGEM	International Center for Global Earth Model

IGS	International GNSS service
INSA	Information Network Security Agency
ITG	Institute of Theoretical Geodesy
ITRF	International Terrestrial Reference Frame
LAGEOS	Laser Geodynamics Satellite
LDHC	Legedadi Health Center
LESL	Legetafo Elementary School
LGO	Leica Geo Office
LIBA	Legetafo International Boarding Academy
MIT	Massachusetts Institute of Technology
MSL	Mean Sea Level
NGA	National Geospatial-Intelligence Agency
PPP	Precise Point Positioning
RL03	Release number three
RMS	Root Mean Square
RSVR	Reservoir
RTX	Real Time eXtended
SGG	Satellite Global Gravity
SLR	Satellite Laser Ranging
SR	Staff Reading
SRTM	Shuttle Radar Topographic Mission
TPS	Theodolite Positioning System
USA	United States of America
US	United states
WGS84	World Geodetic System 1984

List of Symbols

h	ellipsoidal height
H	orthometric height
g	gravity of the Earth
N	geoid height
φ	geodetic latitude
ϕ'	geocentric latitude
λ	longitude
ΔH	change of height
u	upper cross-hair reading
m	middle cross-hair reading
l	lower cross-hair reading
r	distance from the Earth's center of mass
e_{CR}	error due to curvature and refraction
α	collimation angle
e_c	Collimation error
D_{BS}	Back sight distance
D_{FS}	Fore sight distance
$\sum$	Summation
V	Gravitational potential
Φ	potential due to the Earth's rotation
W	Gravitational potential of Earth
C	misclosure
c	speed of light
GM	Geocentric Gravitational Constant

G	universal gravitational constant
M	mass of the Earth
n , m	degree and order respectively
$\bar{S}_{nm}, \bar{C}_{nm}$	fully normalized sine and cosine spherical harmonics coefficients
$\bar{P}_{nm}(sin\phi')$	fully normalized associated Legendre function
a	semi major axis of the WGS84 ellipsoid
ω_e	Earth's rotation rate
W_0	Potential of geoid
∇	gravity gradient
dn	differential path along the perpendicular
c_p	geopotential number of point p
W_p	Potential at point p
γ_0	normal gravity
$\mathrm{H}_{\mathrm{p}}^{\mathrm{dyn}}$	dynamic height of point P
γ_{45}	normal gravity at mid latitude
dH	differential element along the plumb line
$\overline{P}$	Base of the plumb line on the geoid
H_{P}	orthometric height on the surface of point P
$\overline{\mathrm{g}}_{\mathrm{P}}$	average value of gravity along the plumb line at point P
$\frac{\partial\gamma}{\partial h}$	normal gravity gradient
$\overline{\mathrm{g}}_{\mathrm{P}}^{\mathrm{prey}}$	average value of gravity along the plumb line using the Prey reduction
ρ	Earth's crust mean density
$\mathrm{H}_{\mathrm{P}}^{\mathrm{Helmert}}$	Helmert orthometric height at point p
H^N	normal height
ξ	quasi-geoid height

R	mean radius of the Earth
$S(\psi)$	Stoke's function
ψ	geocentric latitude with weights provided by Stoke's function
Δg	gravity anomaly
$P_n(cos\psi)$	associated Legendre polynomial
f	frequency
$d\sigma$	an infinitesimal surface element of the unit sphere σ
t_e	satellite signal emission time of the satellite
t_r	Satellite signal reception time of the receiver
δt_r	clock error of receiver
δt_s	clock error of satellite
$R_r^s(t_r, t_e)$	Pseudorange from satellite to receiver
$\Omega_r^s(t_r, t_e)$	geometric distance between satellite and receiver as a function time
ε	error
β_r^s	ambiguity related to receiver r and satellite s
Υ_r	phase of receiver oscillator
Υ^s	signal phase of satellite
$\omega(n)$	Butterworth filter
$T_{xx}, T_{yy}, T_{zz}, T_{xz}$	gravity gradient components
T	disturbing potential
δg	gravity disturbance
U_0	normal potential on the reference ellipsoid
Λ	Wavelength
U	normal gravity potential

Chapter 1

1. Introduction

1.1 Background

Geodetic Vertical control network provides height information for geodetic, civil engineering, geophysics, geodynamics, geoscience and oceanographic applications. Determining precise vertical positions or heights of points on the surface of the earth is very crucial to define a good national geodetic vertical control network. Height determination is one of the most fundamental measurement types in geodesy and geodetic related sciences. Basically orthometric height is determined from levelling tied to a known bench mark tide gage station. Heights from levelling only provide relative heights between the connected points rather than their absolute heights. Since mean sea level varies at local, regional and global scale due to the changes in the earth's mass redistribution caused by global warming; the typical approach of defining height relative to tide gauge station does not provide a unified and absolute height system in a global sense (Hipkin 2002, Bedada 2010).

Moreover, levelling is time consuming operation and levelled heights are also exposed to both systematic and personal errors. With the advancement of Global Navigation Satellite System (GNSS) and improvement in global gravity models from geodetic satellites missions, there is a growing demand to use gravimetric approach to determine an absolute height of any particular field point on or above the Earth's surface. The approach is to compute geopotential height or geoid height from measurements of gravity field combined with global Earth Gravity Models using Stoke's like integration. Therefore, accurate knowledge of the gravitational potential of the Earth, on a global and regional scale is required with good spatial resolution.

There are numerous uses of global geopotential model having high degree potential coefficients (Tscherning, 1983). One is that, over land areas, Global Navigation Satellite System (GNSS) and gravimetrically determined geoid heights offer the possibility of determining orthometric heights and height differences without the need for levelling (Schwarz et al., 1987).

Even though the spectral combination approach to the geopotential models is different, there are two high resolution geopotential models having spherical harmonic coefficients complete to degree and order of 2190. The first one is the 2008 Earth Gravitational Model EGM2008 which is released by the US National Geospatial Intelligence Agency (Pavlis et al., 2008) and the second is the EIGEN-6C4 gravity field model (Förste et al., 2014). EIGEN-6C4 is the latest combined global gravity field model of Geo Forschungs Zentrum (GFZ) Potsdam and Groupe Recherches Geodesie Spatiale (GRGS) Toulouse. There are many other geopotential models each having its own spherical harmonic coefficients completes to some degree and order. Different models are available at international center for global earth model [ICGEM] website at *http://icgem.gfz-potsdam.de/ICGEM.*

For any geopotential models to be used for geodetic activities anywhere on the globe, it is fundamental to evaluate its accuracy using several independent validation data sets such as geoid heights through the combination of GNSS/levelling heights, airborne and local surface gravity measurements, marine geoid heights from mean oceanographic surface topography models and altimetry observations among others (Kotsakis et al., 2008 and Kılıçoğlu et al., 2008).

Bedada (2010) developed new approach of determining vertical reference system and evaluated the accuracy of the model from Addis Ababa to Adama 100km baseline. Besides, three validation experiments were done at different parts of Ethiopia (Waktola, 2013), (Derese, 2013) and (Worku, 2013) using independent GPS/levelling data. Still there is a need to evaluate the accuracy of the existing models EGM08, GOCO03S and the newly released model EIGEN-6C4 due to this fact, this study aims to further evaluate the two models i.e. EIGEN-6C4 and GOCO03S combined with EGM08 using GNSS-levelling data at different geographic location where the previous models are not evaluated.

1.2 Statement of the problem

Currently, in Ethiopia orthometric heights are determined by conducting differential levelling tied to the nearest first or second order geodetic vertical network bench marks. These bench marks are connected to tide gage stations located at the port of Alexandria, Egypt. Classical levelling approach by its nature is very time consuming and prone to accumulation of systematic and random errors for very long distance between reference point and the new point. First order geodetic bench marks in Ethiopia are not well distributed nor precisely known for their location. It is very expensive and time consuming operation to carryout geodetic levelling in areas where there are no bench marks. Besides, levelling over long baseline introduces significant error budget degrading the accuracy of levelled heights. It is also difficult to carry out sprit levelling to desired point over remote areas which are having rugged topography like most parts of Ethiopia.

Currently, Information Network Security Agency (INSA) has engaged in an effort to modernize the national geospatial infrastructure through observation of the landscape using aerial photogrammetric payload camera. The acquisition of aerial photographs and georeferencing of aerial photos onto geodetic reference system requires the establishment of ground control points (GCP) using GNSS stations at the aerial photogrammetric field survey project area. In relation to this, accurate Digital Elevation Model (DEM) i.e. a series of X, Y, Z coordinates or latitude, longitude and height (H) that accurately portray ground elevations having physical meaning will be prepared if and only if there is orthometric height information of the desired tie points that are collected and adjusted simultaneously with known ground control points during aerial triangulation – orthometric heights shall be determined at GCPs . The generated DTM will be used for of digital orthophoto production.

The application of both rural and urban cadastre requires the determination of orthometric heights at GCPs where GNSS measurements are made. Consequently, Bedada (2010) has developed a new geopotential vertical reference system for Ethiopia to predict orthometric height from geopotential model and GNSS technique at any field point on the surface of the earth where GNSS measurement is available.

But, the accuracy of this geopotential model is not sufficiently assessed over the entire region of Ethiopia. To use geopotential model for practical geodetic applications, it is required to evaluate adequately the accuracy of geopotential model. Therefore, the study aims to evaluate the accuracy of two high resolutions geopotential models synthesised using different spectral combination scheme.

1.3 Objective of the research

1.3.1 General objective

The accuracy of global Earth Gravitational Model (EGM) varies regionally due to availability and quality of local gravity data incorporated during the model development. Hence, the performance of any EGM needs to be validated at a regional scale. Therefore, the general objective of this study is to evaluate the accuracy of EIGEN-6C4, and GOCO03S and EGM08 combined Earth's Gravity Model across a 10.742 km levelling baseline from Addis Ababa to Legedadi using independent GNSS-levelling data.

1.3.2 Specific objective

- To compare EIGEN-6C4 orthometric height with the one computed from GOCO03S and EGM08.
- To compare orthometric height from EIGEN-6C4, and GOCO03S combined with EGM08 with levelled height.
- To evaluate relative accuracy between EIGEN-6C4 geoid height and geoid derived from GOCO03S and EGM08.
- To assess the accuracy of geoid heights derived from EIGEN-6C4, and GOCO03S and EGM08 with geoid height computed from GNSS-Levelling.

1.4 Study area

The accuracy evaluation of Earth Gravity Models: EIGEN-6C4, and GOCO03S combined with EGM08 were carried out by utilizing KARALLO bench mark tied with the existing first order Blue Nile geodetic vertical control bench mark for starting differential levelling work. The study carried out differential levelling across the main asphalt road between Addis Ababa city (Capital of Ethiopia) and Legedadi town covering a total of 10.742 km levelling base line. Five GNSS-levelling bench marks have been selected by reconnaissance so that the selected points will be very suitable for GNSS observation.

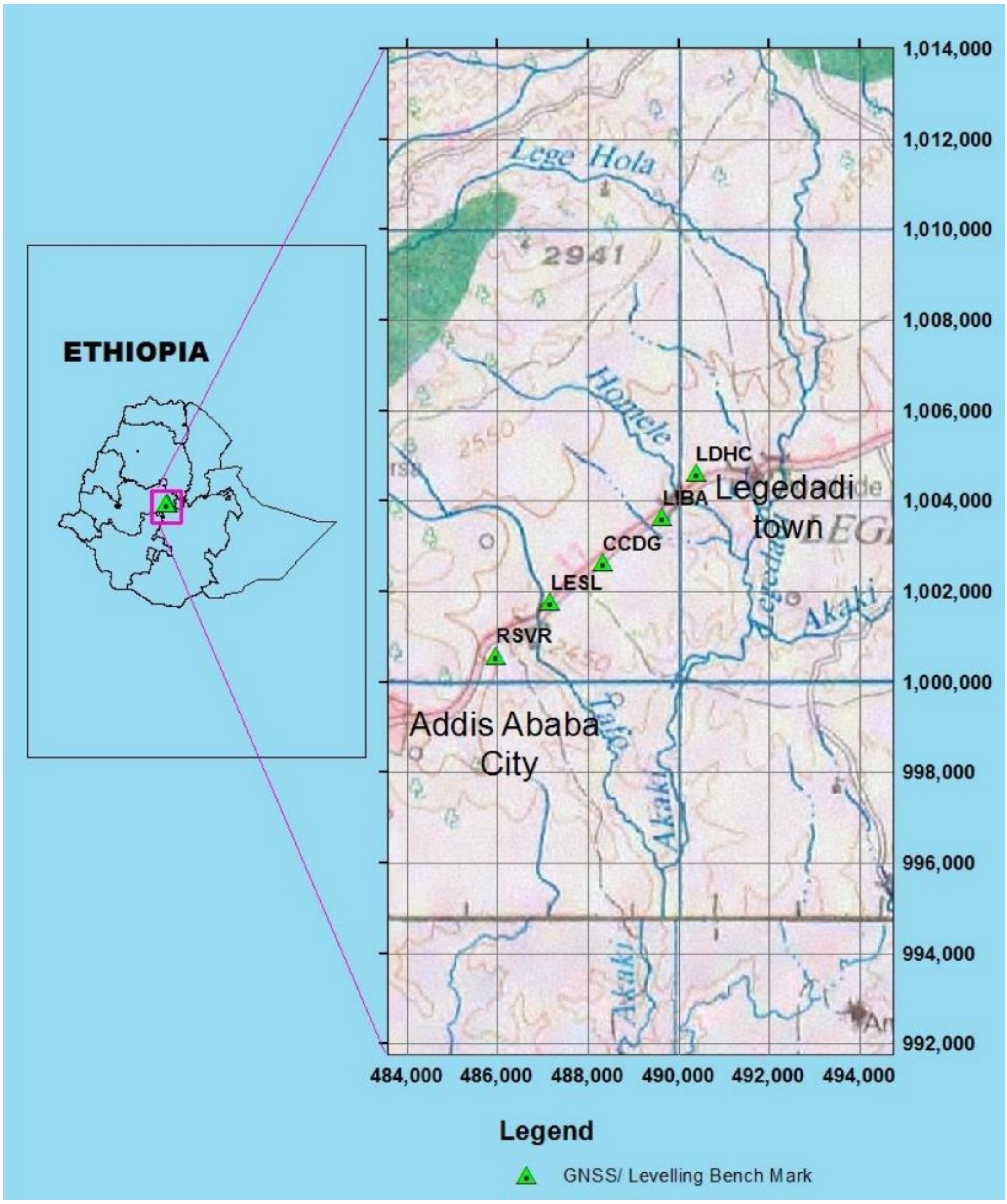

Figure 1. 1: Location of GNSS/Levelling bench mark

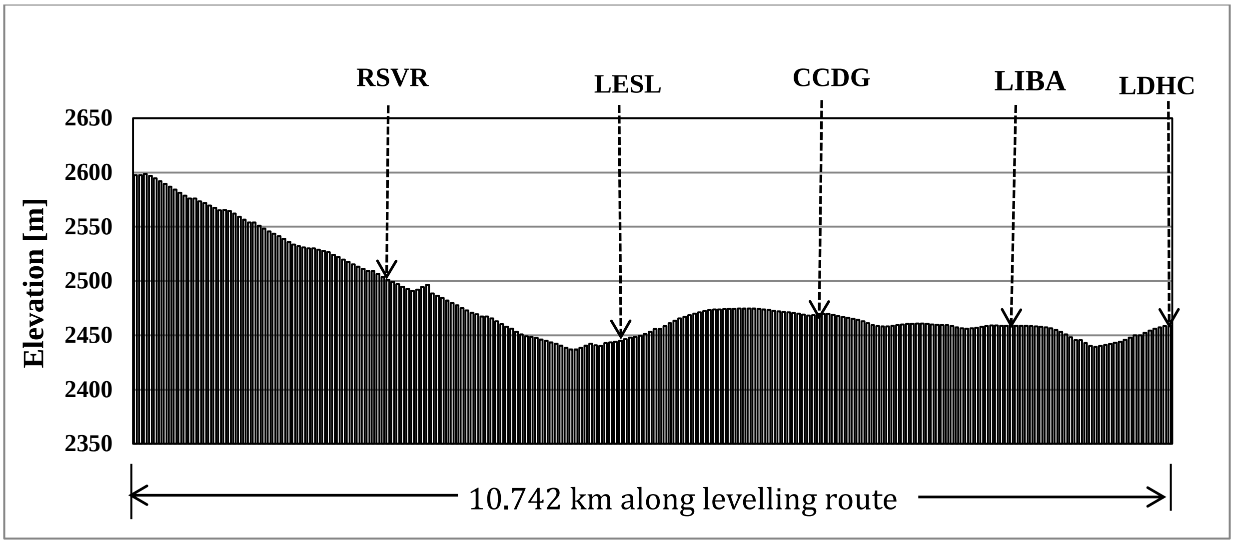

Figure 1. 2: Longitudinal section of differential levelling route profile

1.5 Thesis organization

The thesis consists of five chapters. Chapter 2 presents review of literatures related to the research. This chapter describes about height system, different forms of heights, methods of geoid determination, and theory of GNSS. Chapter 3 deals with the data and methods used for the study. Chapter 4 discusses the main results of the study. Chapter 5 gives conclusions drawn from the findings, and recommendations for future works.

Chapter 2

2. Literature Review

2.1 Height systems

In geodesy, the height of any field point is measured in reference to a zero-height datum usually called the geoid. The geoid is an equipotential surface that globally best fits to the Mean Sea Level. Height is a displacement in distance along the direction of gravitational field and it can be tempting to treat height as the vertical coordinate z, in addition to the horizontal coordinates x and y. However, there is a clear distinction between height and z coordinate. Height has a physical meaning and it defines level surface while z-coordinate is purely a geometrical displacement of any field point with respect to the geocenter orienting along the Earth's axis of rotation. Heights can be measured from different reference surface. Orthometric heights are measured along the direction of gravity above the geoid of mean sea level whereas ellipsoidal heights are measured from the surface of the reference ellipsoid along the direction of ellipsoidal normal.

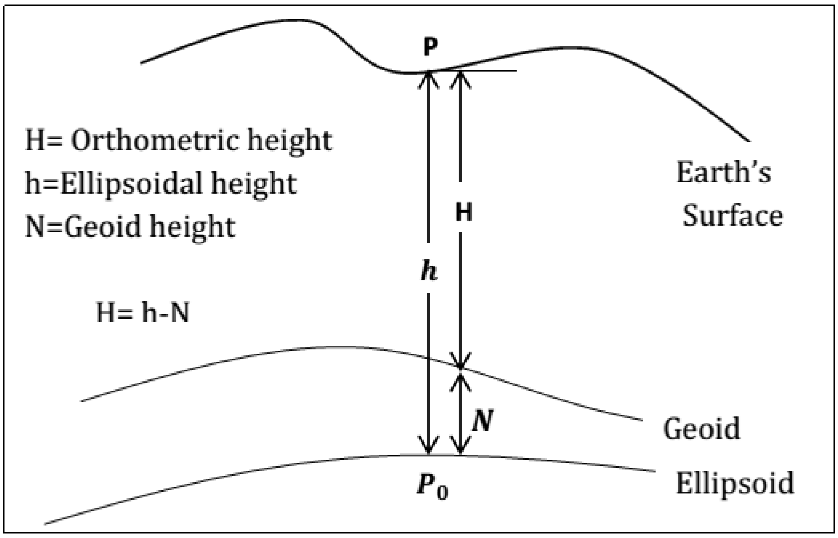

Figure 2. 1: Relationship between H, h and N

Every point on or near the Earth's surface can be uniquely described in terms of three geometrical coordinates called latitude (φ), longitude (λ) and ellipsoidal height (h) – the navigation satellites system provide positioning service in real-time. The latitude and longitude tied to an oblate ellipsoid of revolution and are designated more precisely as geodetic latitude and longitude. This ellipsoid is a geometric mathematical figure that is chosen in some way to fit the mean sea level either globally (WGS84) or locally over some region of the Earth's surface. For WGS84 ellipsoid the origin is fixed at the Earth's center of mass and its minor axis is aligned with the Earth's reference pole. The height of a point P above the reference ellipsoid is called ellipsoidal height (h) . In most geodetic applications, the height of a point should refer to mean sea level or more precisely to a vertical datum which is well-defined reference surface for heights that is accessible at least at one point, called the origin point (Geoid). The ellipsoid is used as the "vertical datum" for ellipsoidal heights which has purely a geometrical meaning. In this case, accessibility is achieved indirectly through the assumption that the ellipsoid is defined in a coordinate frame established by the satellite observations that yield the latitude, longitude and ellipsoidal height of a point. Many geodetic applications involve three different surfaces, which should be clearly defined. The first of these is the Earth's topographic surface. This surface includes the familiar landmass topography as well as the ocean bottom topography. The second is a mathematically manageable reference surface (an ellipsoid) approximating the broad features of the figure of the Earth that does not recover geometric irregularities caused by density variations and topographic undulation. Reference ellipsoids are useful for positioning, navigation, cartography, etc. The third is an equipotential surface of the gravity field of the Earth, called the geoid which is fundamental for geodetic, civil engineering, hydrographic, geophysics, geoscience, and geodynamics applications.

2.2 Methods of determining height

2.2.1 Classical approach

Levelling is the process by which the geometric height difference along the vertical is transferred from a reference station to forward station. The elevation of a point is its vertical distance along plumb line direction above or below a reference level, called datum. The most commonly used datum is the mean sea level (M.S.L). The vertical direction is parallel to the direction of gravity (g) at any point; it is the direction of a freely suspended plumb-bob cord or string. The vertical distance of a point above or below a given reference surface is called the elevation or sometimes (altitude, height, and grade) of the point. Levelling is the general term applied to any of the various processes by which elevations of points or differences in elevation are determined. It is a vital operation in producing necessary data for mapping, engineering design, and construction (Ghilani and Wolf, 2012).

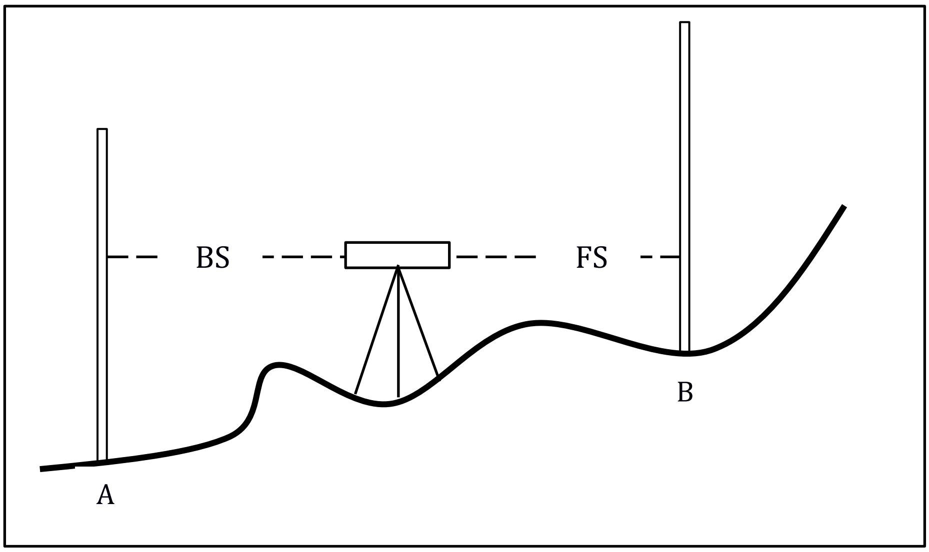

Figure 2. 2: Basic principle of levelling

$$\Delta \mathrm{H} = \mathrm{BS} - \mathrm{FS} \tag{2.1}$$

Where, ΔH is elevation between point A and point B. BS is back sight reading on staff at known point A and FS is fore sight reading on staff at unknown point B.

One of the classical approaches of determining height is differential levelling. Differential levelling principles and errors and modelling methods in levelling will be described in the following sections.

2.2.1.1 Differential levelling

Differential levelling is used to determine differences in elevation between points that are remote from each other by using level, graduated staff and level road. The level consists of cross hair equipped telescope and attached sprit level tube which is mounted on tripod. If the level has been properly set up the telescope which revolves around the vertical axis will give line of site over the horizontal cross hair that defines horizontal plane (Kavanagh and Glenn, 2000). Figure 2.3 below shows *Principle of differential levelling where S1, S2 and S3 are setups.*

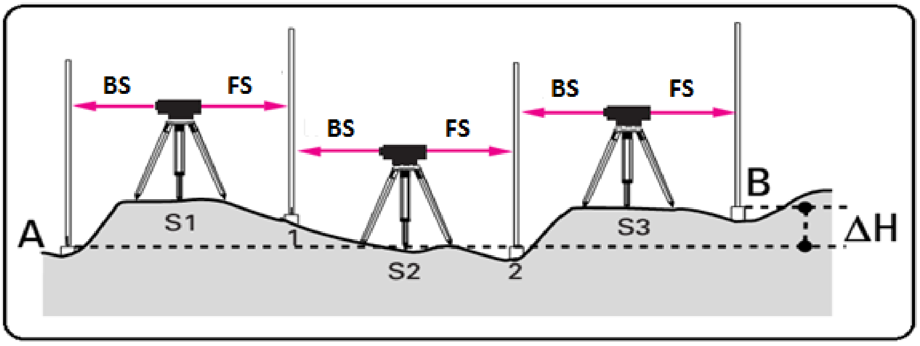

Figure 2. 3: Principle of differential levelling

In differential levelling three-wire levelling method can be employed. As implied by its name, three-wire levelling consists in making rod readings on the upper, middle, and lower crosshairs. The method has the advantages of providing checks against rod reading blunders, producing greater accuracy because averages of three readings are available, and furnishing staff measurements of sight lengths to assist in balancing back sight and foresight distances. In the three-wire procedure the difference between the upper and middle readings is compared with that between the middle and lower values. They must agree within one or two of the smallest units being recorded (usually 0.1 or 0.2 of the least count of the rod graduations); otherwise the readings are repeated (Ghilani and Wolf, 2012). An average of the three readings is used as a computational check against the middle wire.

$$SR = \frac{u + m + l}{3} \tag{2.2}$$

Where SR is average staff reading and u, m, l are upper, middle and lower crosshair reading respectively. The rod readings on the upper, middle, and lower crosshairs are averaged and multiplied by the instrument stadia interval factor gives the sight distances. The difference between back sight and fore sight gives elevation between the two points. Errors associated with the measurements such as collimation, refraction and curvature can be also corrected. This study used three wire differential levelling to establish levelled height across 10.742 km baseline with a tie to the Ethiopian Mapping Agency's bench mark connected to the Bule Nile bench mark. The collimation error is minimized by balancing the distance between back sight and fore sight using steel tape and taping depending on the topography. Levelled heights can also be determined using reciprocal and trigonometric levelling methods (See, Scofield and Breach, 2007).

2.2.1.2 Errors and modelling method in levelling

Differential and trigonometric levelling are the two most commonly employed procedure for finding elevation difference between stations. Both of these methods are subject to systematic and random errors. The primary systematic errors include Earth curvature, atmospheric refraction, and instrument maladjustment (Ghilani and Wolf, 2006). The effects of these systematic errors can be minimized by following proper field procedures. They can also be modelled and corrected computationally. The random errors in differential and trigonometric levelling occur in instrument levelling, booking, and reading graduated scales. These must be treated according to the theory of random errors. One of the systematic errors in differential levelling is collimation error which occurs when the line of sight of an instrument is not truly horizontal and is minimized by keeping sight distances short and balanced. The other systematic error is the effect of refraction and earth's curvature.

As the line of sight extends from an instrument the level surface curves down and away from it. This condition always causes rod readings to be too high. Similarly, as the line of sight extends from the instrument, refraction bends it toward the Earth surface, causing readings to be too low. The combined effect of Earth curvature and refraction on an individual sight always causes a rod reading to be too high by an amount. Fundamentally errors occurred due to systematic error can be minimized keeping back sight and fore sight distance balanced. However, for differential levelling that employs successive number of set ups, correction can be taken by the following expressions.

$$e_c = \alpha\left(\sum D_{BS} - \sum D_{FS}\right) \tag{2.3}$$

Where, e_c is the error in elevation due to the presence of a collimation error and α is collimation angle. The collimation error determined from Equation (2.3) is treated as a correction and thus subtracted from the observed elevation difference to obtain the corrected value. Refraction and earth's curvature error associated with a successive differential levelling survey is given by.

$$e_{CR} = \frac{CR}{1000^2}\left(\sum D_{BS}^2 - \sum D_{FS}^2\right) \tag{2.4}$$

Where e_{CR} is error inroad reading due to earths curvature and refraction and CR = 0.0675 when D is in metres and the error is subtracted from the elevation difference observed. The cumulative effect of systematic errors due to collimation, refraction and earth's curvature on elevation differences can be generally expressed as:

$$e_c + e_{CR} = \alpha\left(\sum D_{BS} - \sum D_{FS}\right) + \frac{CR}{1000^2}\left(\sum D_{BS}^2 - \sum D_{FS}^2\right) \qquad (2.5)$$

Whatever corrections are applied in differential levelling, it is always the levelling circuits fail to close which is called loop misclosure. It is the difference of elevation of the measured or computed elevation and known or established elevation of the same point (Chandra, 2005). The Federal Geodetic Control Subcommittee (FGCS) recommends the following formula to compute allowable misclosure:

$$C = m\sqrt{K} \qquad (2.6)$$

Where C is the allowable loop misclosure, in millimetres; m is a constant; and K is the total length levelled, in kilometres.

For "loops" (levelling circuits that begin and end on the same benchmark), K is the total perimeter distance, and the FGCS specifies constants of 4, 5, 6, 8, and 12 mm for the five classes of levelling, designated, respectively, as (4) first-order class I, (5) first-order class II, (6) second-order class I, (8) second-order class II, and (12) third-order(Ghilani and Wolf, 2012).

2.2.2 Gravimetric approach

In modern geodesy physical heights are determined from measured gravity field of the earth. In the following sections Stoke's method of geoid determination and space domain spherical harmonic analysis are presented.

2.2.2.1 Stoke's method

In 19th century most important formula of physical geodesy was published by George Gabriel Stokes in 1849 (Stokes, 1849). Stoke's formula makes it possible to determine the geoid height (N) from gravity data. However, in its original form the formula only applies for a reference ellipsoid that has the same potential as the geoid, encloses a mass that is numerically equal to the Earth's mass and has its centre at the centre of gravity of the Earth (Hofmann-Wellenhof and Moritz, 2005). The integration in stoke's formula must be carried out over the whole Earth, which requires complete coverage of gravity data over the entire Earth surface. This is not possible as gravity data currently covers only parts of the Earth's surface which necessitates that the area of integration be limited to a spherical cap around the computation point. The formula published by stoke's to determine geoid from gravity anomaly is given as:

$$N = \frac{R}{4\pi\gamma_0}\iint_{\sigma} \Delta g S(\psi) d\sigma \tag{2.7}$$

Where N is geoidal undulation (geoid height), Δg is gravity anomaly, γ_0 is normal gravity, R is mean radius of the spherical earth, $d\sigma$ is an infinitesimal surface element of the unit sphere σ and $S(\psi)$is stoke's function which can be written as:

$$S(\psi) = \frac{1}{\sin(\frac{\psi}{2})} - 6\sin\left(\frac{\psi}{2}\right) + 1 - 5cos\psi - 3cos\psi \ \ln(sin\frac{\psi}{2} + sin^2\frac{\psi}{2}) \tag{2.8}$$

To determine the geoid height (N), Stokes' formula integrates the gravity anomaly (Δg) over the mean Earth sphere of radius R and ψ is geocentric latitude with weights provided by Stoke's function, which can be written in spectral form as:

$$S(\psi) = \sum_{n=2}^{\infty} \frac{2n+1}{n-1} P_n(cos\psi) \tag{2.9}$$

Where $P_n(cos\psi)$ are associated Legendre polynomials (zonal harmonics).

The convectional formula for synthesizing the geoid from free air anomaly components of the global gravity model gives geoid errors with the range of one meter and generates spontaneous geoid slope whose size is very significant (Hipkin, 2002). If a proper global ellipsoidal correction is applied to the Stoke's integral, a geoid with the accuracy of a few millimetres can be achieved. The advantage of this method is that the geoid is level surface, capable of a simple definition in terms of the physically meaningful and geodetically important potential (W_0). The geoid represents a level surface that best approximates mean sea level and it serves as a reference datum for defining physical heights that are measured in meter. The disadvantage is that the potential W inside the earth and hence potential of the geoid W_0 = constant, depends on the density ρ because of Poissons equation ($\Delta W = -4\pi G\varrho + 2\omega^2$). Therefore, in order to determine or use geoid, the density of the mass at every point between the geoid and the ground must be known.

2.2.2.2 Space-domain Spherical harmonics analysis

Modern Geodesy determines the geopotential number directly from a geopotential model expressed in terms of Stoke's dimensionless cosine and sine coefficients. The geopotential number C_P at a point defined by geodetic coordinates φ, λ, h is given by:

$$c_P(\varphi, \lambda, h) = W_0 - W(\varphi, \lambda, h) \tag{2.10}$$

This approach of computing geopotential number involves the task of determining $W(\varphi, \lambda, h)$. The potential W_0 of the geoid can also be computed the global gravity field models .The determination of W_0 and $W(\varphi, \lambda, h)$ from the global gravity model involves space domain spherical harmonic analysis using earths geopotential. This study has used spherical harmonic analysis to determine geoid and geopotential heights from the two geopotential models i.e. EIGEN-6C4, and GOCO03S combined with EGM08. First, the regular grid of disturbing potential δT is computed at different layers (0, 500,1000,…,4000m) ellipsoidal heights and the normal potential of the removed reference ellipsoid is restored to compute the gravitational potential W and the Geopotential heights, at the desired field point on or above the earth surface (Hofmann-Wellenhof and Moritz, 2005). The Potential $W(\varphi, \lambda, h)$ of the field point can be computed from the spherical harmonic coefficients using the following formula.

$$W(\varphi, \lambda, h) = \frac{GM}{a}\left[1 + \sum_{n=2}^{\infty}\left(\frac{a}{r}\right)^{n+1} \sum_{m=0}^{n} \bar{P}_{nm}(cos\phi')(\bar{C}_{nm}\cos m\lambda + \bar{S}_{nm}\sin m\lambda)\right] \tag{2.11}$$

Where,

GM is Geocentric Gravitational Constant

G is universal gravitational constant ($G = 6.67259 \times 10^{-11}\ m^3\ kg^{-1}\ sec^{-2}$ and

M is mass of the Earth ($M=5.972 \times 10^{24}kg$)

r is distance from the Earth's center of mass

a is semi major axis of the WGS84 ellipsoid

n,m are degree and order respectively

ϕ' is geocentric latitude

λ is geocentric longitude which is equal with geodetic longitude

$\bar{S}_{nm}, \bar{C}_{nm}$ are fully normalized sine and cosine spherical harmonics coefficients

$\bar{P}_{nm}(cos\phi')$ is fully normalized associated Legendre function

2.3 Earth's Geopotential

The geopotential is the gravitational potential generated by the masses of the Earth, including its atmosphere. In addition, the potential from other masses in the solar system may be considered separately, especially that of the sun and moon, as they introduce a time-varying field due to their apparent motions relative to the Earth. The Earth's total geopotential W is defined as:

$$\mathrm{W} = \mathrm{V} + \Phi \tag{2.12}$$

Where

V is the gravitational potential

Φ is the potential due to the Earth's rotation

The gravitational potential V, is expressed most conveniently in terms of spherical harmonic functions (an alternative formulation in terms of ellipsoidal harmonics is also sometimes used). The gravitational potential function V is defined as:

$$V = \frac{GM}{r}\left[1 + \sum_{n=2}^{n_{max}} \left(\frac{a}{r}\right)^n \sum_{m=0}^{n} (\bar{C}_{nm}\cos m\lambda + \bar{S}_{nm}\sin m\lambda)\bar{P}_{nm}(sin\phi')\right] \tag{2.13}$$

Fully normalized associated Legendre function can be written in equation form as:

$$\bar{P}_{nm}(\sin\phi') = \sqrt{\frac{(n-m)!\,(2n+1)G}{(n+m)!}} \times P_{nm}(\sin\phi') \tag{2.14}$$

As it is expressed in equation (2.12) Earth's total geopotential can be derived from gravitational acceleration and rotational acceleration. Because of Earth's rotation, static gravimeters on the Earth experience a centrifugal acceleration that (because of Einstein's Equivalence Principle) cannot be distinguished from the effect of gravitation. Similarly, it is convenient to define a centrifugal potential that generates the centrifugal acceleration as:

$$\Phi = \frac{1}{2}\omega_e^2 r^2 \sin^2\phi' \tag{2.15}$$

Where, ω_e is Earth's rotation rate

The relationship between the gravity vector and its potential is:

$$\mathbf{g} = \nabla\mathbf{W} \tag{2.16}$$

Where, ∇ denotes gradient operator.

Gradient is vector pointing in the direction of steepest descent of a function that is the vector perpendicular to the equipotential surfaces.

The component of gravity perpendicular to the equipotential surface thus represents its magnitude and we may write it as:

$$|\mathbf{g}| = \mathrm{g} = -\frac{\mathrm{dW}}{\mathrm{dn}} \tag{2.17}$$

Where, dn is a differential path along the perpendicular and the minus sign is a matter of convention (potential decreases with altitude, path length is positive upwards, and gravity magnitude is positive.

2.4 Geopotential Height

Geopotential height is defined as energy difference between the potential of the geoid and the potential of a particular field point on or above the earth's surface. This energy difference or geopotential height is equal to the work done by the conservative gravitational force along the path length projected in the direction of gravity field. This is given by evaluating the Stokes like integral (Heiskanen and Moritz, 1967). Geopotential height or geopotential number is used to trace a level or equipotential surface on the earth's surface through a GNSS coordinate (φ, λ, h). Equipotential surfaces are closed and continuous surfaces with a unique constant gravity potential value W.

2.4.1 Dynamic height

Any point has geopotential height with respect to the geoid, and this itself appropriately scaled, can be used as a height coordinate of the point. Dynamic height is defined as geopotential of any point on the surface of the earth scaled to the normal gravity γ_0 at 45 degree latitude. Specifically, for an adopted constant γ_0 we can have:

$$\mathrm{H_p^{dyn}} = \frac{\mathrm{c_p}}{\gamma_0} = \frac{\mathrm{c_p}}{\gamma_{45}} \tag{2.18}$$

$\mathrm{H_p^{dyn}}$ is the dynamic height of P with respect to vertical datum and $\mathrm{c_p}$ is geopotential number/height of point P. The scale factor is usually chosen as a nominal value of gravity at mid-latitude (γ_0) or (γ_{45}) = 9.806199203 m/s^2; GRS80 value, Moritz, 1992).

Scaling geopotential numbers by constant does not change their fundamental property, so dynamic height produce equipotential surface.

2.4.2 Orthometric height

Orthometric height is the distance along the plumb line between the geoid and the point located on the earth's surface (Hofmann-Wellenhof and Helmut Mortiz, 2005). Orthometric heights are measured in meters and have physical meaning telling us the direction of uphill and downhill. It is measured along the direction of plumb line and perpendicular to equipotential surfaces. From geopotential number and gravity, mathematically orthometric height can be expressed as:

$$H_P = \frac{c_P}{\bar{g}_P} \qquad 2.19$$

Where, H_P is orthometric height on the surface of point P, c_P is geopotential umber of point P and $\overline{g}_P$ is average value of gravity along the plumb line at point P.

2.4.3 Helmert orthometric height

Helmert in 1890 used Poincar$\acute{e}$-pray's gravity gradient for the definition of orthometric height.According to this approach the gravity value needed for the evaluation of the height is obtained from the observed gravity at the earth's surface reduced to mid-point between earth's surface and the geoid, considering the gravity gradient is constant along the plumb line. The average value of gravity along the plumb line is given as:

$$\bar{g}_P = \frac{1}{H_P}\int_{\bar{P}}^{P} g dH \qquad (2.20)$$

The value of $\overline{g}_P$ cannot be computed exactly using Newton's Law of Gravitation because this would require complete knowledge of the mass density of the crust and it is not practical to measure g along the plumb line. Therefore, in theory, the orthometric height cannot be determined exactly, and its calculation depends on some density hypothesis, or model, for the crust. In essence, the determination of the orthometric height depends on the approximation used in computing the mean value of gravity evaluated between the geoid and the point P (Hofmann-Wellenhof and Moritz, 2005). The average gravity along the plumb line, between and P_0 and P, is obtained using the Prey reduction. This reduction models the value of gravity inside the crust by first removing a Bouguer plate of density, applying a free-air downward continuation using the normal gradient of gravity, and restoring the Bouguer plate. Each of these operations is linear in H_P; and, consequently, the average value of gravity along the plumb line is simply the average of the endpoint values of gravity. The general equation for Helmert orthometric height can be formulated as:

$$H_P^{Helmert} = \frac{c_P}{\bar{g}_P^{prey}} = \frac{c_P}{g_p + 0.0424H_p} \tag{2.21}$$

Where, c_P is in g.p.u (geopotential unit), g_p is in gal and H_p is in km

This equation is solved by iterations due to the fact that the computation of gravity along the plumb line always requires H_P information (Hofmann-Wallenhof and Moritz, 2005; Jekeli, 2000).

2.4.4 Normal height

In practice pure orthometric heights cannot be realized due to the requirement to measure gravity inside the topography. To avoid this problem, in 1945 Molodensky (Molodensky, 1962) introduced the concept of normal heights and the corresponding surfaces i.e. the telluroid and the quasi - geoid.

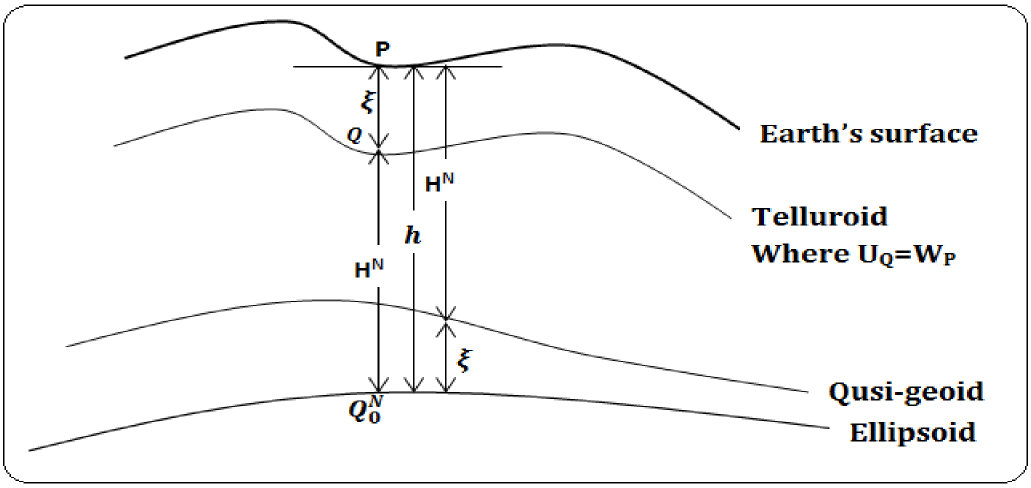

Figure 2. 4: Normal height (H^N), Quasi-geoid height (ξ) and ellipsoidal height (h)

The normal height of point P on the Earth's surface H^N can be defined as the vertical distance measured along the normal gravity plumb line from the reference ellipsoid (point Q_0^N) to the telluroid (point Q). Clearly this definition introduces a new surface i.e. the telluroid which is not coincident with the Earth's surface and is also not an equipotential surface like the geoid. However, following the Molodensky theory the telluroid is considered as the surface on which the normal potential U_Q at every point Q is equal to the actual potential W_P at the corresponding point P on the Earth's surface which is $U_Q = W_P$, provided P and Q are situated on the same ellipsoidal normal (Hofmann-Wellenhof and Moritz, 2005). As an integral, the normal height of point P on the Earth's surface is defined by (Heiskanen and Moritz, 1967) as:

$$\mathrm{H^N} = \frac{\mathrm{c_P}}{\overline{\gamma}} \tag{2.22}$$

Where $H^N$is normal height, $\overline{\gamma}$ is the mean normal gravity along the ellipsoidal normal through point P and given by (Heiskanen and Moritz, 1967) as:

$$\overline{\gamma} = \gamma\left[1 - (1 + f + m - 2f sin^2\varphi_P)\frac{H^N}{a} + \left(\frac{H^N}{a}\right)^2\right] \tag{2.23}$$

γ is normal gravity on the ellipsoid at the point of computation ,f is the geometrical flattening of the ellipsoid ,m is the geodetic parameter (ratio of gravitational and centrifugal force at the equator), $\varphi_P$is the geodetic latitude of point P.

Alternatively normal heights can be determined by subtracting quasi-geoid/height anomaly from ellipsoidal height:

$$H^N = h - \xi \tag{2.24}$$

Where $H^N$is normal height, h is the ellipsoidal height determined by GNSS, ξ is the quasi-geoid height, that is, the distance measured along the ellipsoidal normal between the reference ellipsoid and the quasi-geoid which by definition is equivalent to the height anomaly i.e. distance estimated along the ellipsoidal normal from point P on the Earth's surface to point Q on the telluroid (Featherstone and Kuhn, 2006).

2.5 The Blue Nile vertical geodetic network of Ethiopia

The Blue Nile vertical control bench marks were established for the purpose of investigating the Blue Nile basin (1957 – 1961). The Blue Nile bench marks are tied to tide gauge station located at the port of Alexandria. The existing Blue Nile Geodetic levelling network start at the port of Alexandria following Nile basin passes along Khartoum and crosses to Ethiopia through Metema - Azozo(Gonder) - Adiszemen – combolcha – kemise - Debrebrehan - Addis Ababa- Ambo – Gimbi - Assosa – Guba – Bahir Dar.

Guba – Bahir Dar levelling line is connected with the levelling line coming from Adiszemen to Bahir Dar. The other levelling line is running from Combolcha – Mile - Semera – Elidar – Aseb (Ethiopia Geodetic survey, 1957-1961).

Blue Nile vertical control bench marks were established along the road and currently most of these bench marks are destroyed due to different reasons like road construction and lack of awareness about the values of the bench marks. Figure 2.4 illustrates the Blue Nile vertical geodetic network distribution (Blackwell, 1962).

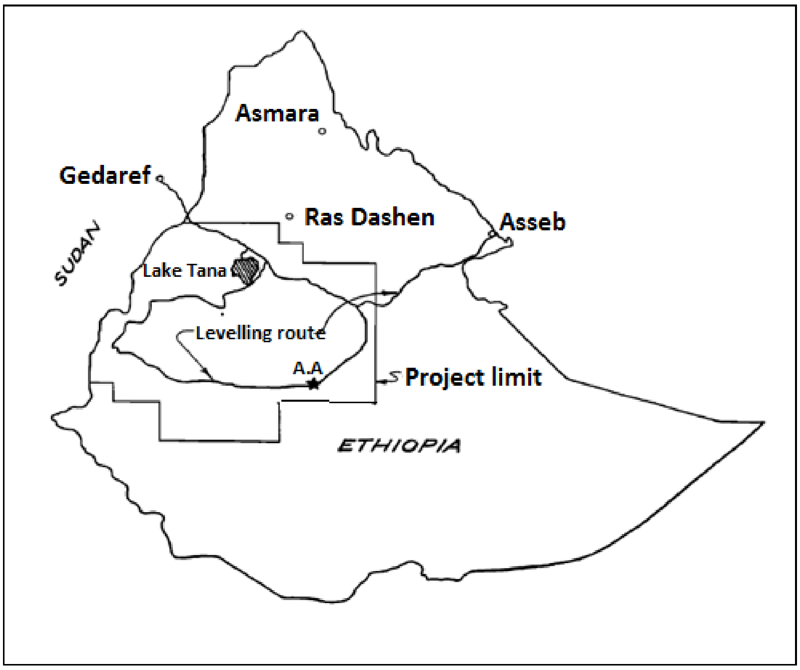

Figure 2. 5: Blue Nile vertical geodetic network

2.6 Geopotential Height System of Ethiopia

2.6.1 Current status

Bedada (2010) develop new approach of determining vertical reference system by incorporating airborne gravity data, the 2008 Earth Gravity Model (EGM08) and geometrical and spherical gravity models of the Shuttle Radar Topographic Mission (SRTM) in a 'Remove-Compute-Restore' process to determine absolute vertical reference system for Ethiopia. This gives a geopotential height at any isolated field point where there is a Global Navigation Satellite System (GNSS) measurement without reference to a vertical network or a regional datum point (Bedada, 2010).

The accuracy of the geopotential number computed from gravity and topography was evaluated by comparing it with the one derived directly from EGM08 and precise geodetic levelling. The new model is in a good agreement across 100 km baseline with a standard deviation of $56\times10^{-2}m^2s^{-2}$and $39\times10^{-2}m^2s^{-2}$ or equivalently (5.6cm and 3.6cm) relative to EGM08 and levelling, respectively (Bedada, 2010).

The new method provides an absolute geopotential height of a point on or above the Earth's surface in a global sense by interpolating from geopotential models prepared as the digital grids carried in a chip for use with the GNSS receiver in the field replacing the classical approach of determining orthometric height using sprit levelling which is time consuming and exposed to different forms of error.

2.6.2 Validation of the new geopotential models

In order to make the new geopotential models be effectively used at national level, the models shall be validated against an independent levelling data. In 2013, three validation experiments were done at Addis Ababa University. This are hybrid model of GOCO03S satellite only and EGM2008 validation in case study of Hageremariam to Yabelo (Waktola, 2013), validation of the new 2008 Earth Gravity Model for Addis Ababa and western part of Ethiopia (Derese, 2013) and validation of the 2008 earth gravity model a case study around Debre Birhan (Worku, 2013) using independent GNSS/levelling data. The mismatches of orthometric heights and from mismatches of geoids are ~2cm and ~2.6cm respectively for Addis Ababa and western part of Ethiopia (Kebie, 2013), the misfit between the levelled heights and gravity based orthometric height has significantly large standard deviation of about 1.8m (Waktola, 2013) and comparison of orthometric height with level height gave the best result with datum offset of -3.73cm between the gravimetric geoid defined by $W_0 - U_0$ and levelling datum(Worku, 2013).

By using Addis Ababa to Adama levelling data GOCO03S and EGM2008 hybrid geopotential model has shown a significant improvement in reducing the vertical datum offset between the level datum and the geoid model from 27cm to 0.04cm with standard deviation of 3.9cm when the long wavelength of EGM2008 is replaced by the GOCO03S gravity model (Waktola, 2013). For the effective use of new model for different geodetic applications over the whole country, validation has to be done across the country in such a way that levelling and GNSS observation has to be done for remaining parts of the country (Waktola, Worku and Kebie, 2013).

2.7 Global Navigation Satellite System (GNSS)

GNSS technique determines three dimensional coordinates of a point on surface of the earth. These coordinates are always calculated with the reference to geocentric ellipsoid. This means that the coordinate obtained will be ellipsoidal rather than orthometric. Orthometric heights can be obtained through differential levelling (See, section 2.2) and derived from GNSS measurement if the precise local geoid of an area is known.

2.7.1 GNSS derived orthometric heights

GNSS surveying techniques have proven to be so efficient and accurate that they are now routinely used in place of classical methods for establishing vertical control networks. Understandably, interest has been growing in using GNSS techniques to replace all levelling requirements. These require accurate geopotential models and tools to facilitate GNSS derived orthometric heights replacing classical approach for many applications. In the meantime, it is important to have a clear understanding of the basic concepts of establishing GNSS-derived orthometric heights, otherwise water may not flow downhill.

Three types of heights are involved in computing GNSS-derived orthometric heights. These are firstly, orthometric height – the distance from the geoidal reference surface to the point, measured along the plumb line normal to the geoid. Secondly, ellipsoid height- the distance from the reference ellipsoid to the point, measured along the line that is normal to the ellipsoid. Thirdly, at the same point on the surface of the Earth, the difference between an ellipsoid height and an orthometric height is defined as the geoid height (N). See figure 2.1 for the relationship between these heights.

Now it is important to describe the relationship between geometric and physical geodesy. Geometrical geodesy is concerned with describing locations in terms of geometry. Consequently, coordinate systems are one of the primary products of geometrical geodesy. Physical geodesy is concerned with determining the Earth's gravity field i.e. necessary for determining physical heights. It deals also with the measurement and representation of the Earth's gravity field. Using GNSS, geometric coordinates φ, λ, h are determined from which geometrical ellipsoidal height (h) is involved in deriving orthometric height which is physically meaningful. This indicates that physical geodesy and geometrical/GNSS geodesy are tied together for providing vertical reference system. In modern theory of geopotential height system realization, physical and geometrical geodesy is inseparable. Therefore, this literature review will focus on basic principles of GNSS positioning and error sources and modelling methods. However, the historical back ground, constellation, signal structure and reference coordinate system of GNSS position is described in detail (See, Xu, 2007).

2.7.2 Basic principles of GNSS positioning

Precise distances from the satellites to the receivers are determined from timing and signal information, enabling receiver positions to be computed. In satellite geodesy, the satellites become the reference or control stations, and the ranges (distances) to these satellites are used to compute the positions of the receiver. Conceptually, its basic principle is equivalent to ***resection*** in conventional ground surveying tasks. The global positioning system architecture can be categorised into three parts these are the space segment, the control segment, and the user segment.

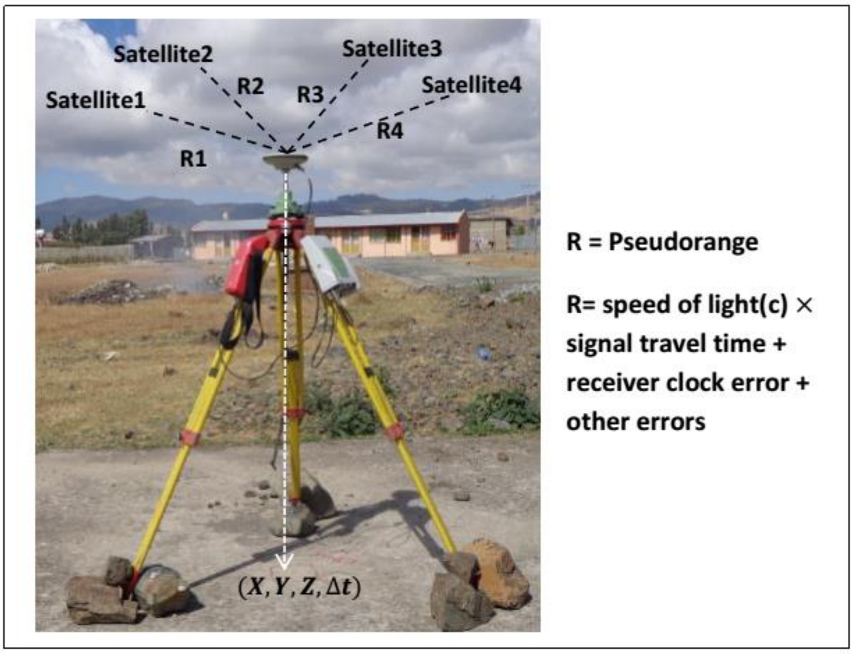

Figure 2. 6: Basic principle of GNSS positioning

2.7.3 Code and Carrier measurements

2.7.3.1 Code Pseudoranges

The pseudorange is a measure of the distance between the satellite and the receiver's antenna. The distance is measured through measuring the signal transmitting time from the satellite to the receiver's antenna. Therefore, such a distance is referred to the distance between the satellite at the time of the signal emission and the receiver's antenna at the time of signals reception. The transmition time is measured through maximum correlation analysis of the receiver code and the satellite signal. The receiver code is derived from the clock used in the receiver. The measured pseudorange is different from the geometric distance between the satellite and the receiver's antenna because of the errors of the both clocks and the influences of the signal transmitting mediums. For vacuum medium and error-free situation, the measured pseudorange is equal to the geometric distance and can be presented by:

$$R_r^s(t_r, t_e) = (t_r - t_e)c \tag{2.25}$$

Where t_e is the signal emission time of the satellite, t_r is signal reception time of the receiver, c is the speed of light and subscript r and superscript s denote the receiver and satellite, respectively. On the lefthand side t_r denotes the epoch at which the pseudorange is measured.

Taking the satellite and receiver clock errors into account, the pseudorange can be represented by the following formula:

$$R_r^s(t_r, t_e) = (t_r - t_e)c - (\delta t_r - \delta t_s)c \tag{2.26}$$

Where, δt_r and δt_s denote the clock errors of the receiver and satellite, respectively. Taking the ionospheric effects, tropospheric effects, Earth tide and loading tide effects, multipath and relativistic effects as well as remaining errors into account, the pseudorange model equation is given as:

$$R_r^s(t_r, t_e) = \Omega_r^s(t_r, t_e) - (\delta t_r - \delta t_s)c + \delta_{ion} + \delta_{tro} + \delta_{tide} + \delta_{mul} + \delta_{rel} + \varepsilon \tag{2.27}$$

Where, $R_r^s(t_r, t_e)$ on the left-hand side is the measured pseudorange which is equals to the geometric distance between the satellite at the emission time and the antenna at the reception time plus or minus several corrections. The above discussed pseudorange model is generally valid for both C/A code and P code.

2.7.3.2 Carrier Phases

The carrier phase is a measure of the phase of the received satellite signal relative to the receiver generated carrier phase at the reception time. The measurement is made by shifting the receiver-generated phase to track the received phase. The number of full carrier waves between the receiver and the satellite cannot be accounted for at the initial signal acquisition. Therefore, measuring the carrier phase is to measure the fractional phase and to keep track of changes in the cycles. The carrier phase observable is indeed an accumulated carrier phase observation. The fractional carrier phase can be measured by electronics with precision better than 1% of the wavelength, which corresponds to millimetre precision (Xu, 2007).This is also the reason why the phase measurement is more precise than that of the code. A full carrier wave is called a cycle. The ambiguous integer number of cycles in the carrier phase measurement is called ambiguity. In the case of a vacuum medium and an error-free situation, the measured phase can be presented by

$$\Upsilon_r^s(t_r) = \Phi_r(t_r) - \Upsilon^s(t_r) + \beta_r^s \tag{2.28}$$

Where, subscript, r and superscript, s denotes the receiver and satellite, respectively, t_r is signal reception time of the receiver, Υ_r is the phase of receiver oscillator, Υ^s is signal phase of satellite and β_r^s is the ambiguity related to receiver r and satellite s.

Taking bath the satellite and receiver error in account, the carrier phase can be replaced as:

$$\Upsilon_r^s(t_r) = \frac{\Omega_r^s(t_r, t_e)f}{c} - f(\delta t_r - \delta t_s) + \beta_r^s \tag{2.29}$$

Where δt_r and δt_s denote the clock errors of the receiver and satellite, respectively. The frequency f and wavelength Λ have the relation of:

$$c = \Lambda f \tag{2.30}$$

Taking the ionospheric effects, tropospheric effects, Earth tide and loading tide effects, multipath and relativistic effects as well as remaining errors into account, the carrier phase model equation (2.29) can be completed as:

$$\Upsilon_r^s(t_r) = \frac{\Omega_r^s(t_r,t_e)}{\Lambda} - f(\delta t_r - \delta t_s) + \beta_r^s - \frac{\delta_{ion}}{\Lambda} + \frac{\delta_{tro}}{\Lambda} + \frac{\delta_{tide}}{\Lambda} + \frac{\delta_{mul}}{\Lambda} + \frac{\delta_{rel}}{\Lambda} + \frac{\varepsilon}{\Lambda} \tag{2.31}$$

Or

$$\Lambda\Upsilon_r^s(t_r) = \Omega_r^s(t_r, t_e) - c(\delta t_r - \delta t_s) + \Lambda\beta_r^s - \delta_{ion} + \delta_{tro} + \delta_{tide} + \delta_{mul} + \delta_{rel} + \varepsilon \tag{2.32}$$

Where, the measured phase on the left-hand side equals the geometric distance between the satellite at the emission time and the antenna at the reception time plus or minus several corrections. The clock error corrections are scaled by the speed of light c.

2.7.4 GNSS positioning errors and modelling methods

The final position of the survey station is influenced by the error in the range measurement, the satellite–receiver geometry, the accuracy of the satellite ephemerides, the effect of atmospheric refraction, the multipath environment at the receivers, the quantity and quality of satellite data collected, the connections between the observed GNSS network and the existing control and processing software used.

It is necessary, therefore, to consider the various errors involved, some of which are already been mentioned above. The majority of the error sources are eliminated or substantially reduced if relative positioning is used rather than single-point positioning. As discussed above in Code and Carrier observables, different errors have been considered and different equations have been also developed from through equation (2.25 to 2.32).

Chapter 3

3. Materials and Method

3.1 Introduction

The method aims to assess the accuracy of two geopotential models such are GOCO03S combined with EGM08, and EIGEN-6C4 along 10.742 km levelling baseline from Addis Ababa to Legedadi. GOCE c-series EIGEN family geopotential model EIGEN-6C4 which is a static global combined gravity field model up to degree and order 2190. Evaluating the accuracy of the two geopotential models requires measuring co-located in-situ levelled heights and geodetic coordinates (latitude, longitude, ellipsoidal height) along the survey baseline. The detailed methodological approach and datasets used in this study will be discussed in-depth in the next sections.

This comprises data collection, processing, analysis, interpretation and comparison. Global Navigation Satellite System [GNSS] data, Earth's geopotential models such as EIGEN-6C4, EGM08 and GOCO03S as well as precise levelling height have been used to conduct this research. Different set of GNSS data processing methods i.e. GAMIT/GLOBK, AUSPOS, Trimble RTX post-processing and Leica Geo Office (LGO) are used for processing GNSS data collected using Leica GS10 and LEICA GX1230+ receivers. Accuracy assessment have been also done for latitude, longitude and ellipsoidal height (φ, λ, h) obtained from different set of data processing methods. In addition to this, errors analysis for φ, λ, h have been done for each GNSS-levelling benchmarks which indicated the magnitude of the error for each set of processing methods and the differences of latitude, longitude and ellipsoidal height are also statically described here in this research to support decision to wards selecting the most promising result φ, λ, h obtained from different methods which will be used for further analysis and computation of geopotential heights using geopotential models.

Utilizing latitude, longitude and ellipsoidal height space-domain spherical harmonic analyses is carried out to compute geopotential number at point P (c_P) and geoid heights (N) directly from the EIGEN-6C4 at GNSS-levelling benchmarks. This modern approach of computing geopotential heights using the global geopotential model involves the task of tracing level surface on the Earth's topography through the ellipsoidal height obtained from any particular field point where GNSS observation is taken (Bedada, 2010).

From EIGEN-6C4 geopotential model geoid height and different geopotential heights at five GNSS-levelling benchmarks namely (RSVR, LESL, CCDG, LIB, and LDHC) established along the main asphalt road between Addis Ababa and Legedadi are computed and related with result obtained from precise levelling height during evaluation.

Accuracy evaluation has been conducted for the combined model [EGM08 & GOCO03S] created by combining GOCO03S satellite only model and EGM08 aimed to compare different forms of geopotential heights derived from EIGEN-6C4 geopotential model. GOCO03S (long wavelength of gravity field) and EGM08 (medium to short wavelength of gravity field) is used to produce hybrid geopotential model (Waktola, 2013). Generating the hybrid model is carried out by truncating the EGM08 and GOCO03S at a frequency of 240 defined to degree 2190 and order 2159.

At the validation phase the research has compared the different geopotential heights and geoid heights obtained from global gravity models i.e. EIGEN-6C4 and hybrid model with geometrically determined precise levelling height and ellipsoidal height from GNSS observation. In addition to this the datum offset of EIGEN-6C4 and the hybrid model is compared to decide which geopotential model has shown improvement in reducing the datum offset between the level datum and geoid model.

3.2 Data used in the analysis

3.2.1 Earth's Geopotential Models

3.2.1.1 Earth Gravitational Model 2008 (EGM08)

The National Geospatial-Intelligence Agency (NGA) of the USA has developed a new Earth Gravitational Model, called EGM08 (Pavlis et al., 2008), and intended to replace the US EGM96 model which served as one of standards for the Earth gravity models. The new gravity model is complete to degree n and order m up to 2160 in the spherical harmonic expansion. It means that, EGM08 can provide a ground resolution of 9 km × 9 km in equatorial region showing substantial improvement over the EGM96 which has provided 55 km spatial resolution at a global scale.

EGM08 is a spherical harmonic model of the Earth's gravitational potential, developed by a least squares combination of the ITG-GRACE03S gravitational model and its associated error covariance matrix, with the gravitational information obtained from a global set of area-mean free-air gravity anomalies defined on a 5 arc minute equiangular grid over the region of ocean using model coefficients, up to degree and order 180 (Mayer-Gürr, 2007). This grid was formed by merging terrestrial, altimetry-derived, and airborne gravity data. Over areas where only lower resolution gravity data were available, their spectral content was supplemented with gravitational information implied by the topography. The accuracy goal for the EGM08 was set to ±15 cm global Root Mean Square (RMS) geoid undulation commission error (Pavlis et al., 2008). Some studies showed that the discrepancies between EGM08 geoid undulations and independent GNSS/levelling data are improved to the order of ±5 to ±10 cm in areas where detailed local gravity data is available (Pavlis et al., 2008 and Bedada, 2010).

In Ethiopia, EGM08 incorporates high resolution airborne gravity data consisting of 92,433 along-track gravity measurements, corresponding to 90,000km flight distance with across-track resolution of 18 km (Bedada, 2010). Moreover, Bedada (2010) developed a rigorous method of computing geopotential height or geoid model by combining geometrical and condensed topographic gravity models and airborne gravity data with EGM08 in a Remove-Compute-Restore approach and he showed that the new geopotential model super pass EGM08 when compared to levelled heights in Ethiopia.

3.2.1.2 Third generation GOCE satellite only [GOCO03S] geopotential model

The GOCO (Gravity Observation Combination) initiative has computed high-accuracy and high resolution global gravity field models from complimentary gravity data sources such as satellite gravity missions GOCE, GRACE, CHAMP, SLR and terrestrial gravity field and satellite altimetry data. GOCO03S is released since 2011 which is the third solution of satellite only gravity model that contains GOCE satellite gravity data after the launch of GOCE satellite since March 17, 2009. GOCO03S was developed from 18 months GOCE data, 7 years of GRACE data, 8 years CHAMP data and 5 years of SLR data (Mayer-Gürr, 2011). The model was expanded up to spherical harmonic degree 250 and Kaula's rule was applied for the regularization of the degrees greater than 180 (ESA, 2012). This model can be downloaded from international center for global earth model [ICGEM] *http://icgem.gfz-potsdam.de/ICGEM*

3.2.1.3 Hybrid geopotential model from EGM08 and GOCO03S

Hybrid global gravity model was produced by combining satellite only GOCO03S with the Earth Gravity Model 2008 (EGM08). The aim of combining these two models is to get wide range of gravity from low frequency to high frequency (Waktola, 2013). In Ethiopia, EGM2008 has good medium to short wavelength of Earth's gravity field as recovered by the Ethiopian airborne gravity survey project (Bedada, 2010). As GOCE is only able to contribute better information from degrees 200 to 240, degree of 240 is used as truncation frequency to combine EGM2008 and GOCO03S geopotential models.

To combine the EGM08 and GOCO03S models, a high pass Butterworth filter of the following form has been used to scale the cosine and sine coefficients of the EGM08 which adds back the filtered coefficients to the low pass filtered GOCO03S coefficients.

The high-pass butter worth filter that is applied to suppress the long wavelengths and enhance medium to short wavelengths of EGM08 model is given in equation 3.1.

$$\omega(n) = 1 - \frac{1}{1 + \left(\frac{n}{n_0}\right)^k} \tag{3.1}$$

The filter is very close to 1 for $n > n_0$ and close to zero for $n < n_0$, with a smooth transition between the two regimes. A large value of k makes the transition more convergent. The values of k = 10 and n_0= 240 are used in this study.

The low-pass filter that is applied to enhance long wavelength components of GOCO03S is given in equation 3.2.:

$$\omega(n)_{low} = 1 - \omega(n) = \frac{1}{1 + \left(\frac{n}{n_0}\right)^k} \tag{3.2}$$

The resulting hybrid geopotential model has got long wavelength from GOCO03S and medium to short wavelength from EGM08. The new hybrid spherical harmonic coefficients are created by using equation 3.3. On top of this, Figure 3.1 shows the combination of the two models in a more simple schematic representation.

$$\begin{pmatrix} C_n^m \\ S_n^m \end{pmatrix} = 1 - \left(w(n)\right) \times \begin{pmatrix} C_n^m \\ S_n^m \end{pmatrix}_{GOCO03S} + \ w(n) \times \begin{pmatrix} C_n^m \\ S_n^m \end{pmatrix}_{EGM2008} \tag{3.3}$$

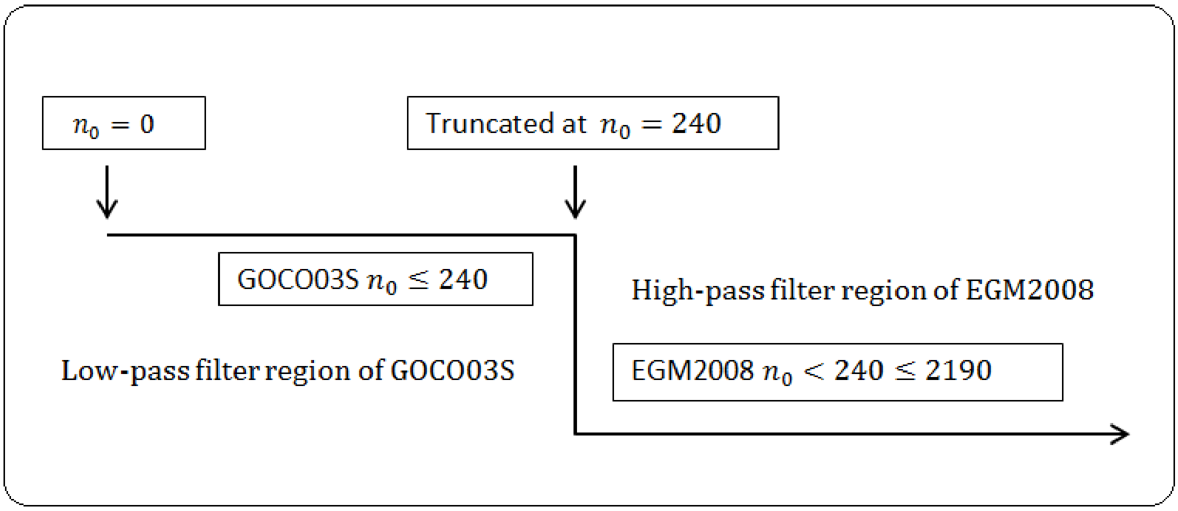

Figure 3. 1: Combination scheme of GOCO03S and EGM2008 geopotential model.

3.2.1.4 EIGEN-6C4

EIGEN-6C4 (European Improved Gravity model of the Earth by New techniques) is a static global combined gravity field model up to degree and order 2190. It is developed jointly by GFZ Potsdam and GRGS Toulouse. The combination of the different satellite and surface data sets has been done by a band-limited combination of normal equations to max degree 370, which are generated from observation equations for the spherical harmonic coefficients (Förste et al., 2014). A brief description of the applied techniques for the generation of such a combined gravity field model is given in (Shako et al., 2014). The resulted solution to degree and order 370 has been extended to degree and order 2190 by a block diagonal solution using the DTU10 global gravity anomaly data grid.

Input data used for combination are LAGEOS (degree 2 - 30) from 1985 – 2010, GRACE RL03 GRGS (degree 2 - 130) from 2003 - 2012 for consecutive ten years, GOCE-SGG data; processed by the direct approach (Pail et al., 2011, Bruinsma et al., 2014) to degree 235 including the gravity gradient components Txx, Tyy, Tzz and Txz out of the following time spans: 837 days out of the nominal mission time span 2009 11 01 – 2012 08 01 422 days out of the lower orbit phase between 20120901 - 20130524 .The GOCE polar gaps were stabilized by the Spherical Cap Regularization (Metzler and Pail , 2005) using the combined gravity field model EIGEN-6C3 satellite and terrestrial data (max degree 370): DTU12 ocean geoid data (see also Anderson et al., 2009 and 2010) and an EGM08 geoid height grid for the continents.

This model can be downloaded from International Center for Global Earth Model [ICGEM] website at *http://icgem.gfz-potsdam.de/ICGEM*. On top of this Figure 3.2 illustrates the overall combination of the EIGEN-6C4 geopotential model.

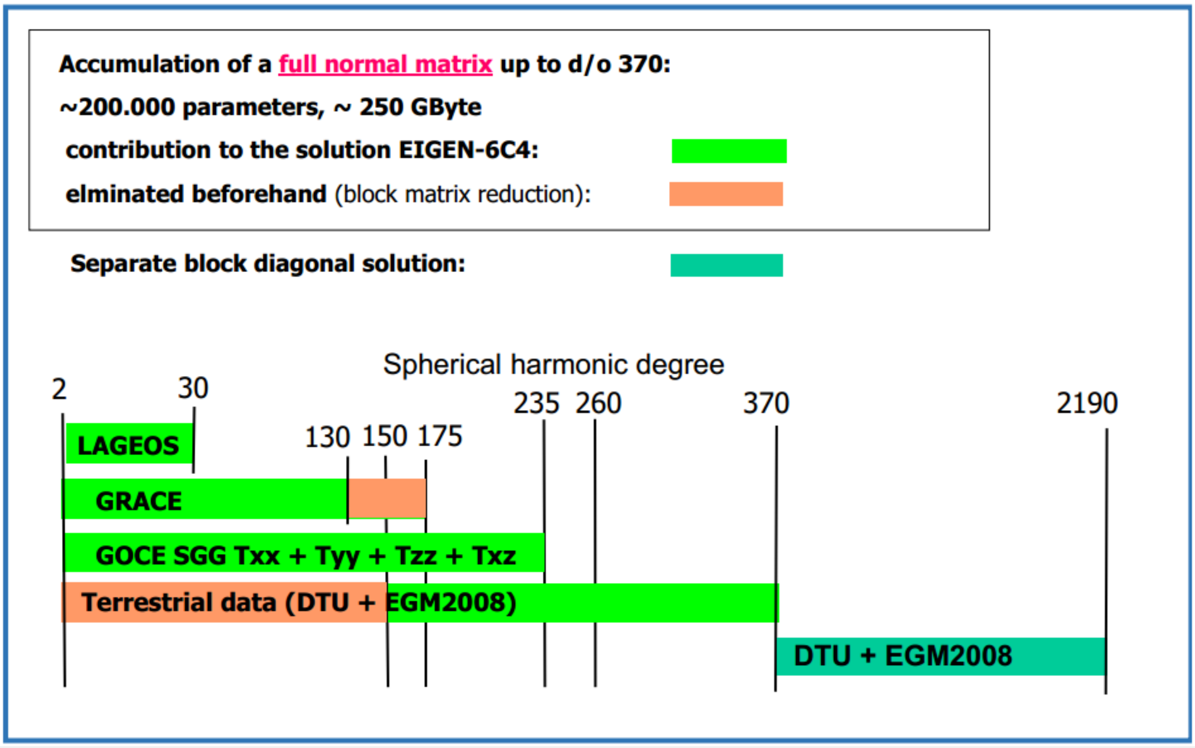

Figure 3. 2: Combination scheme of the normal equation for EIGEN-6C4 geopotential model. [Source: 5th GOCE user workshop presentation Christian-Alberchts University, Paris, November 2014]

3.3 GNSS Data Collection and Processing methods

3.3.1 GNSS Data Collection

GNSS data is one of the independent fundamental data sets required to validate the accuracies of hybrid (GOCO03S and EGM08) and EIGEN-6C4 geopotential models. For the purpose of geopotential models evaluation, the GNSS data were collected for 72 hours at five GNSS/levelling bench marks from 15 December 2016 to 21 December 2016. In other words, the GNSS data are measured on Day Of Year spanning from DOY350 to DOY355. The names of the GNSS/levelling bench marks for which GNSS data were measured are RSVR, LESL, CCDG, LIBA and LDHC. These bench marks are located along the asphalt road from Addis Ababa to Legedadi. The bench marks were established at about 2km interval; taking in to account the GNSS signal obstruction and reliability of the station with regard to future road renewal and expansion projects. Leica brand GPS receivers were used to collect the data at each bench mark. The description of receivers and antenna information used at each station is given in Table 3.1 below.

Table 3. 1: GNSS receivers and antenna information used at each bench mark.

Station Name: CCDG	
GNSS receiver information	
Receiver Serial number	1531683
Receiver ART number	771510
Receiver (equipment) number	4240068
Receiver Type	LEICA GS10
Antenna serial number	10481047
antenna ART number	770701
Antenna product number(P/N)	01018431
Antenna Type	LEIAS10

Station Name: LIBA	
GNSS receiver information	
Receiver Serial number	1531678
Receiver ART number	771510
Receiver (equipment) number	4240063
Receiver Type	LEICA GS10
Antenna serial number	11381116
antenna ART number	770701
Antenna product number(P/N)	01018431
Antenna Type	LEIAS10

Station Name: LDHC	
GNSS receiver information	
Receiver Serial number	1531683
Receiver ART number	771510
Receiver (equipment) number	4240068
Receiver Type	LEICA GS10
Antenna serial number	10481047
antenna ART number	770701
Antenna product number(P/N)	01018431
Antenna Type	LEIAS10

Station Name: LESL	
GNSS receiver information	
Receiver Serial number	1531678
Receiver ART number	771510
Receiver (equipment) number	4240063
Receiver Type	LEICA GS10
Antenna serial number	11381116
antenna ART number	770701
Antenna product number(P/N)	01018431
Antenna Type	LEIAS10

Station Name: RSVR	
GNSS receiver information	
Receiver Serial number	480951
Receiver ART number	766711
Receiver (equipment) number	3525299
Receiver Type	LEICA GX1230+
Antenna serial number	09110023
antenna ART number	766714
Antenna product number(P/N)	01018147
Antenna Type	LEIAX1203+GNSS

At each GNSS station data has been acquired at 15 seconds data logging rate and then resampled to 30 seconds interval during processing phase with reference to the selected IGS stations. In addition to this, the cut-off angle for navigation satellites visibility is set to 15°- data is gathered only from navigation satellites with elevation angle greater than 15°. This is because observations to low elevation satellites can sometimes be problematic and may result in data with low accuracy with possibility in causing data loss due to radio signal obstruction. . Furthermore, if there are problems with the resolution of ambiguities, an increase in the cut–off angle might also improve processing; because the removal of the noisier data from low elevation satellites can reduce the overall phase noise. This ensures that there still remains sufficient data with a good Geometric Dilution of Precision (GDOP).

Figure 3. 3: Leica GS10 GNSS receiver observing data at station LDHC.

All necessary information were recorded to the GNSS observation site log sheet before starting observation and after ending observations to ensure accurate information about antenna and receiver that are needed while processing of the observed GNSS data. At each site, geodetic latitude, longitude and ellipsoidal height were measured in reference to the 1984 World Geodetic System (WGS84).

3.3.2 GNSS Data Processing packages and services

This study has processed GNSS data using different software packages such are GAMIT/GLOBK, Leica Geo Office, Real Time eXtended (RTX) and AUSPOS.

GAMIT is a comprehensive GPS Analysis package developed at Massachusetts Institute of Technology (MIT) and Scripps for the estimation of three-dimensional relative positions of ground stations or for estimating station coordinates and velocities, satellite orbits, and Earth orientation parameters. GLOBK is a Kalman filter whose primary purpose is to combine solutions from the processing of primary data from space-geodetic or terrestrial observations and used to plot the residual in three dimensions.

Leica Geo Office (LGO) is the office software; which accompanies the LEICA viva series. It supports all measurement types (TPS, GNSS and Level data) and ideal tool to view, process, and quality-check and archive data before exporting it to virtually any format required by subsequent mapping or engineering software packages (Leica Geo Office home page). For this study we used Leica Geo Office version 7.0.

RTX is a GNSS online data processing service that is based on real-time kinematic (RTK) and precise point positioning (PPP) in a technique that does not require local reference stations, while still providing the high productivity and accuracy of RTK systems with the extended coverage area of solutions based on global satellite corrections (Chen et al., 2011). RTX uses innovative positioning and compression algorithms to compute and satellite orbit, satellite clock, and other system adjustments and transmit corrections to receivers via satellite and IP providing accurate geodetic coordinates.
In this study rinex data was submitted to the RTX post-processing service at www.trimblertx.com/uploadform.

On the other hand, AUSPOS is also an online GNSS data processing facility provided by geoscience Australia and is based on **Bernese** software. AUSPOS uses International GNSS Service (IGS) products (final, rapid, ultra-rapid depending on availability) to compute precise coordinates in ITRF08 anywhere on Earth designed to process only dual frequency GNSS phase data with reference to International Terrestrial Reference Frame (ITRF08) coordinates. Usually, users will submit their dual frequency geodetic quality rinex data observed in a 'static' mode to online AUSPOS service and receive a summary report via e-mail.

For this study, we used AUSPOS 2.2 and Bernese version 5.2. *(www.ga.gov.au/scientific-topics/position-navigation/geodesy/auspos).*

Our method of getting good quality GNSS data is based on comparing the accuracies of the results from the four processing software packages. GNSS solutions with highest accuracy will be used for geopotential height computation and for the evaluation of GNSS/levelling data. The detail of this evaluation will be discussed in chapter four.

3.4 Levelling data

Precise levelled heights are one of the fundamental data that are commonly used to assess the accuracy of geopotential models. Levelled heights are determined by carrying out differential levelling with a tie to a known existing levelling network. For this study, levelled heights were collected along the main asphalt road from Addis Ababa to Legedadi (see, Figure 3.4). Levelling network covered a total of 21,667.700m including forward and backward levelling. Levelled heights were determined at five bench marks that were established at a separation of 2km. The levelled heights were connected to the existing KARALLO bench mark (See, Annex B) owned by the Ethiopian Mapping Agency (EMA). The KARALLO levelling bench mark is tied to the historical tide gauge mean sea level datum located at the Alexandria port of Egypt through the Blue Nile levelling bench marks. Each Blue Nile vertical control bench marks are established along road (Ethiopia Geodetic Survey, 1957-1961).

Figure 3. 4: Levelling crew conducting differential levelling.
[From Left to right: Zewudu Hailu, Mohammednur Abdela, Zerihun Geremew and Tofik Ali]

3.5 Determination of geoid and orthometric height

Stokes' formula makes it possible to determine the geoid height from gravity data . Gravity disturbances and anomalous potential from a global gravity models described by fully normalized spherical harmonics are used to compute geopotential heights. Space - domain spherical harmonic analysis directly computes the geopotential height from a set of dimensionless Stoke's cosine and sine coefficients. Determinations of such physical heights are directly related with normal gravity γ_0 measured above reference ellipsoid and disturbing potential T as described in stokes integral (Stokes, 1849). Typically, the calculation of geoid height from gravity data will use a detailed coverage of gravity anomalies in the region where the geoid height is needed as well as in a broad track of surrounding territory. However, integral like stokes function is global so the gravity data set ought to be cover the whole Earth. But, modern physical geodesy compiles surface gravity data and satellite based gravimetry into a global gravity model described as a series of spherical harmonic coefficients. It then constructs gravity residuals by removing the effect of the level ellipsoid, the effect of the topographic masses and a contribution from a global gravity model. For the latter, the spherical harmonic series is truncated of tapered at some degree where it is anticipated that shorter wavelengths are given more accurately by local gravity observations. The “Tg_Schmidt” and “Tg_Interp” FORTRAN programs are used for the computation of geopotential height from hybrid (GOCO03S and EGM08) and EIGEN-6C4 geopotential model. Computation of disturbing potential is basically related to theory of gravitational potential V (See, equation 2.13).

The anomalous potential T can be determined using the following equation (Hofmann-Wellenhof and Moritz, 2005).

$$T = \frac{R}{4\pi}\iint_{\sigma}\Delta g S(\psi) d\sigma \tag{3.4}$$

By Burns formula geoid height (N) is defined as disturbing potential (T) scaled to normal gravity as:

$$N = \frac{T}{\gamma_0} \tag{3.5}$$

By substituting equation (3.5) in to (3.6) Stokes integral is determined which is used to compute geoid height (N).

$$N = \frac{R}{4\pi\gamma_0}\iint_{\sigma}\Delta g S(\psi) d\sigma \tag{3.6}$$

Gravity disturbance which is the negative gradient of the disturbance potential in the radial direction is give as

$$\delta g = \frac{-\partial T}{\partial h} \tag{3.7}$$

Other program called “Tg_interp” is used to estimate orthometric heights at GNSS observation points from pre-computed regular grids of disturbing potential and gravity disturbance at different heights (0, 500m, 1000m, 1500m ..., 4500m) at every 500m intervals above the reference ellipsoid. In practice of orthometric height computation, first disturbing potential is calculated at GNSS observation point. Then the normal potential of the reference ellipsoid is added to the disturbing potential to get the gravity potential $W(\varphi,\lambda,h)$. This gives the geopotential number (c_P) at GNSS observation point by subtracting the potential $W(\varphi,\lambda,h)$ from the potential of the geoid and this can be expressed in the following equation.

$$c(\varphi,\lambda,h) = W_0 - W(\varphi,\lambda,h) \tag{3.8}$$

Orthometric height can be computed from equation (3.8) by scaling geopotential number by the mean value of the gravity along the plump line between the geoid and the field point.

$$H = \frac{c(\varphi, \lambda, h)}{\bar{g}} \tag{3.9}$$

The mean gravity ($\bar{g}$) can be estimated from regular grids of gravity disturbance or gravity anomaly.

In this study different forms of heights such as normal height, Helmert orthometric height, were determined by scaling geopotential number by different forms of mean values of gravity between the geoid and the surface field points as well as by subtracting geoid height and telluroid from ellipsoidal height.

Figure 3.5 illustrates the overall methodological scheme applied in this study to assess the accuracy of geopotential height using GNSS-levelling data.

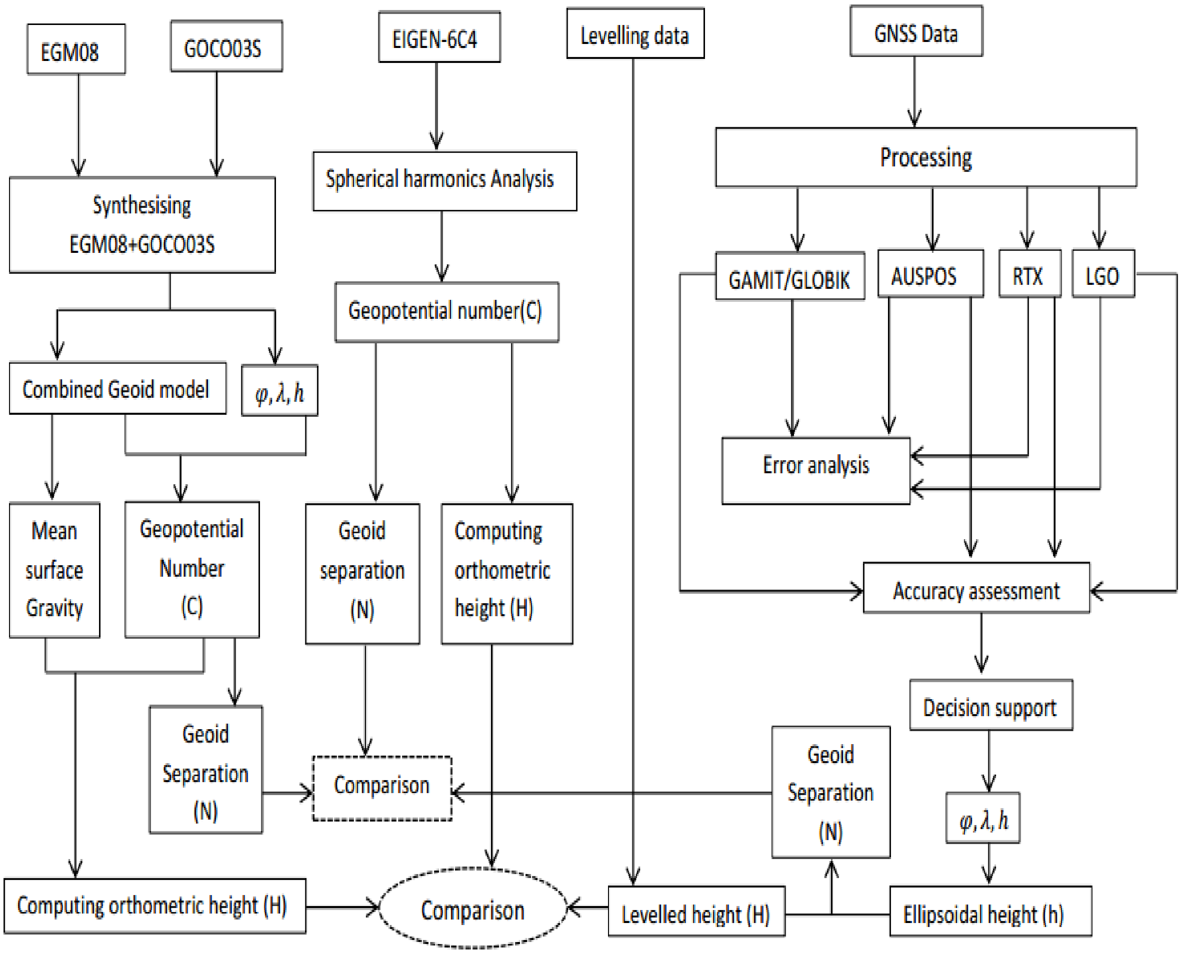

Figure 3. 5: Scheme of methodological approach.

Chapter 4

4. Results and Analysis

4.1 Results of GNSS data processing

Receiver INdependent EXhange(RINEX) data was processed for each GNSS-levelling benchmark station using different software packages as described in chapter three. The data was processed with respect to the 1984 world geodetic system (WGS84) reference frame using IGS orbit product precise ephemeris.

4.1.1 Gamit/Globk

The coordinates for each of the GNSS-levelling benchmark were computed using GAMIT for the respective days accurate to mm in latitude, longitude and ellipsoidal height with a tie to WGS84 reference ellipsoid. All the coordinates were computed relative to seven IGS network stations such are Ethiopia (ADIS), Kenya (MOIU, MAL2), Italy (NOT1), Israel (DRAG), Iran (THEN), ZAMBIA (ZAMB) and GABON (NKLG). The stations were chosen based on proximity to the local benchmarks and stability based on the velocity solutions as presented in ITRF08.

Figure 4. 1: IGS stations used in Gamit/Globk.

Globk was used to compute the average of the solutions obtained using GAMIT as well as plot the residuals for computed coordinates. Computed coordinates are described in Table 4.1 below and also (See, Annex A) for IGS stations coordinates.

Table 4. 1: Geodetic coordinates of the local stations computed using Gamit/Globk.

Station	Latitude in degrees	Longitude in degrees	Height(h) in meter	Standard deviation in meter		
				Latitude	Longitude	Height(h)
CCDG	9.072482937	38.89480107	2463.615	0.003	0.003	0.011
LIBA	9.081534555	38.90668322	2452.603	0.003	0.003	0.012
RSVR	9.053909065	38.87318459	2476.808	0.003	0.003	0.011
LDHC	9.090434796	38.91337623	2461.219	0.004	0.003	0.012
LESL	9.064676644	38.88412970	2453.404	0.004	0.004	0.013

In addition to computing the average solutions for each station in the network, Globk is capable of plotting the residuals for the computed coordinates.

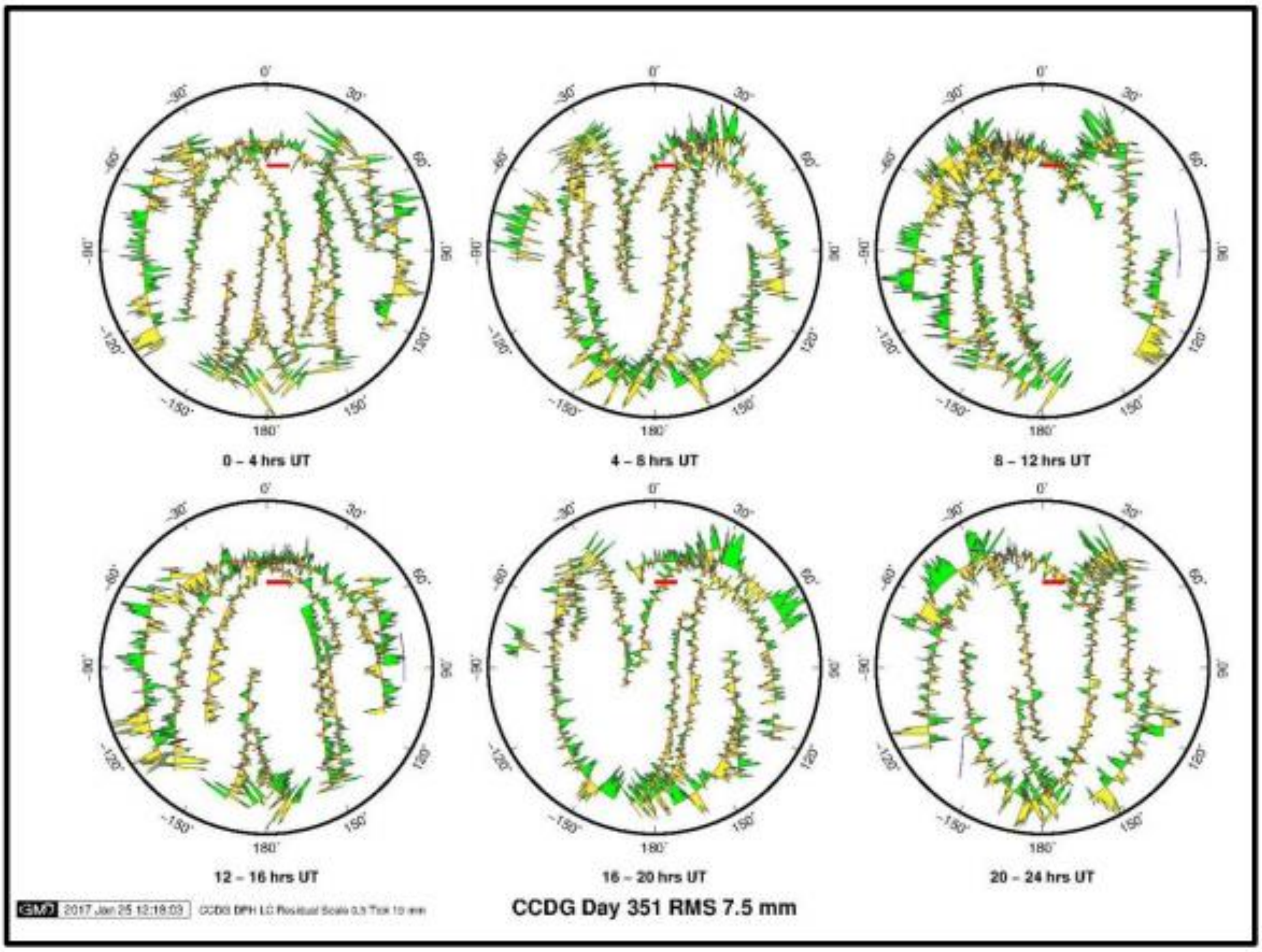

Figure 4. 2: Sky plot of station CCDG for DOY351.

Figure 4.2 illustrates the sky plots for station CCDG on DOY351 has good geometry of satellites distribution. This good geometry of satellites gives good information for the receiver. Also, there is no multipath effect occurred on the receiver because there is no any common effect that can be observed at the same direction for different satellites.

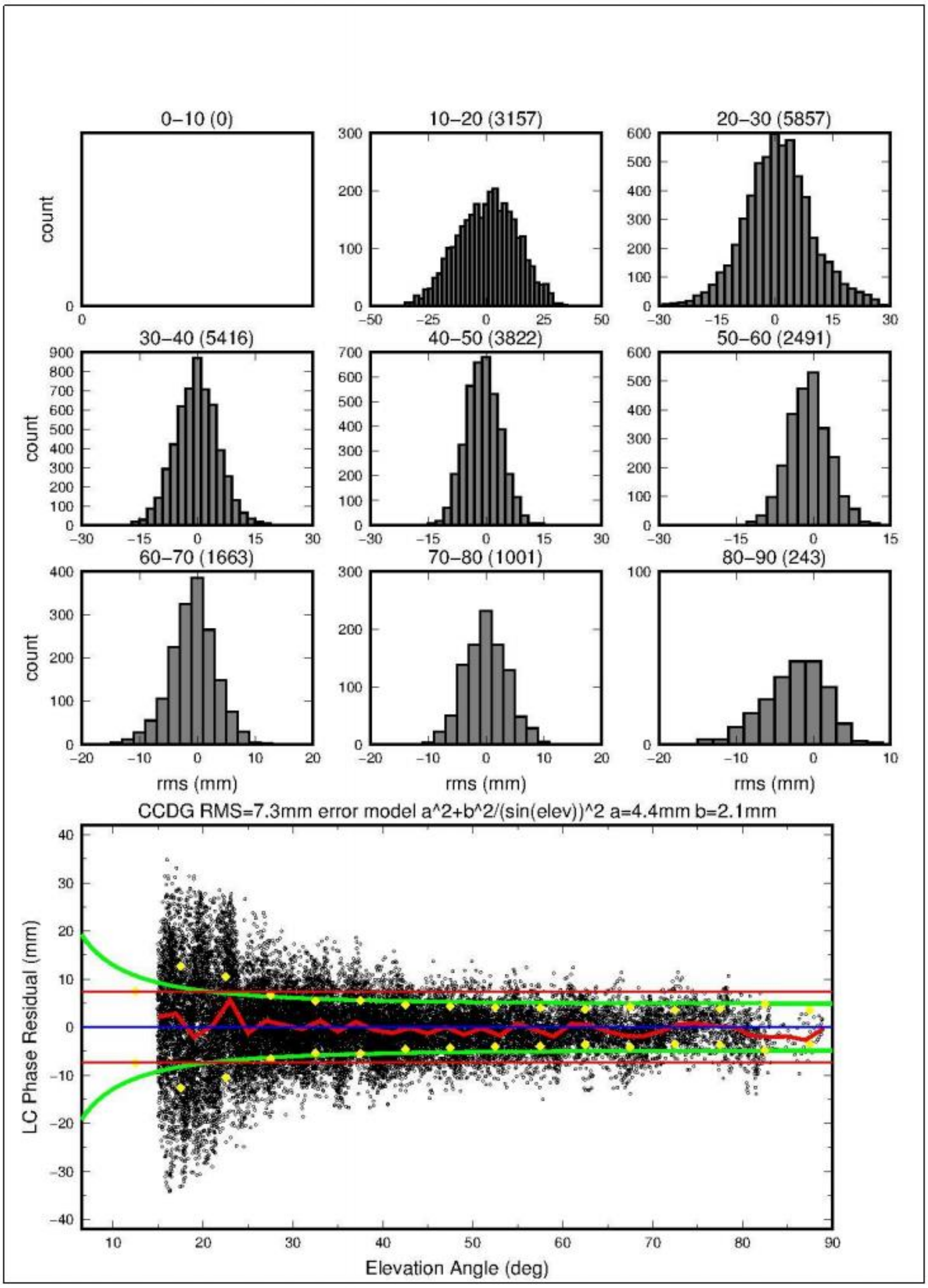

Figure 4. 3: LC residual versus Elevation angle plot at CCDG bench mark.

The plot of phase residual versus elevation angle has normal pattern showing the stability of station at every elevation angle (Figure 4.3). Red lines are smoothing of individual values and show no strong systematic error. Green lines show the elevation dependent noise model and used to re-weight the data. The phase versus elevation angle plot also shows that physical performance of this station is slightly good and stable.

4.1.2 AUSPOS-Processing service

While using this service, RINEX data was submitted for each DOY and the data was processed and submitted via e-mail. Results from each report are compiled and average to get latitude, longitude and ellipsoidal height coordinates of each GNSS-levelling bench. Data processing and measurement modelling phase pre-processing is undertaken in a baseline by baseline mode using triple-differences (Auspos report, page 5). In most cases, cycle slips are fixed by the simultaneous analysis of different linear combinations of L1 and L2. If a cycle slip cannot be fixed reliably, bad data points are removed or new ambiguities will be resolved based on weighted post-fit residuals and outliers are removed. In estimating station coordinates, coordinate constraints are applied at the reference sites with standard deviation of 1mm and 2mm for horizontal and vertical components respectively. All the coordinates were computed relative to seven IGS network stations such as Turkey (ANKR and ISTA), Cyprus (NICO), Italy (NOT1), Israel (DRAG), Iran (THEN) and Zambia (ZAMB).The stations were chosen automatically by the service package (Figure 4.4).

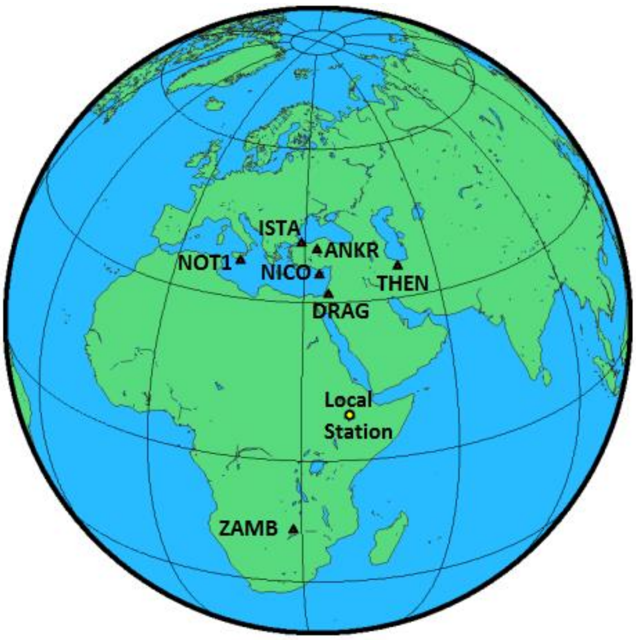

Figure 4. 4: IGS stations used in AUSPOS-Processing

This Processing service uses International GNSS Service (IGS) products (final, rapid, ultra-rapid depending on availability) to compute precise coordinates in ITRF anywhere on Earth. In this study dual frequency phase data has been processed using final IGS products that are available in the system.

Table 4. 2: Geodetic coordinates of the local stations derived based on AUSPOS-processing.

Station	Latitude in degree	Longitude in degree	Height(h) in meter	Standard deviation in meter		
				Latitude	Longitude	Height(h)
CCDG	9.072482957	38.89480117	2463.633	0.005	0.006	0.013
LIBA	9.081534567	38.90668331	2452.620	0.005	0.006	0.013
RSVR	9.053909089	38.8731847	2476.829	0.005	0.006	0.013
LDHC	9.090434844	38.91337641	2461.229	0.005	0.006	0.013
LESL	9.064676697	38.88412987	2453.476	0.005	0.006	0.014

4.1.3 Real Time eXtended (RTX)

GPS RINEX data of the local bench marks are processed using Post-Processing Service Based on RTX Technology. The data were processed in ITRF2008 at epoch 2005.0 and ITRF2008 at epoch 2016.96 (Table 4.4). The output of the processing includes the coordinates of the bench marks and list of satellites used for adjustment of the solutions (Table 4.3).

Table 4. 3: Results of bench mark LIBA derived from observations taken for doy350-352.

Used Satellites

# Total Satellites:	54
GPS:	G01 G02 G03 G05 G06 G07 G08 G09 G10 G11 G12 G13 G14 G15 G16 G17 G18 G19 G20 G21 G22 G23 G24 G25 G26 G27 G28 G29 G30 G31 G32
GLONASS:	R01 R02 R03 R04 R05 R06 R07 R08 R09 R10 R11 R13 R14 R15 R16 R17 R18 R19 R20 R21 R22 R23 R24

Processing Results

ITRF2008 at Epoch 2005.0		
Coordinate	**Value**	**σ**
X	4903351.798 m	0.005 m
Y	3957450.177 m	0.005 m
Z	1000454.946 m	0.002 m
Latitude	09° 04' 53.51595" N	0.001 m
Longitude	38° 54' 24.05003" E	0.003 m
El. Height	2452.618 m	0.006 m

ITRF2008 at Epoch 2016.96		
Coordinate	**Value**	**σ**
X	4903351.581 m	0.005 m
Y	3957450.383 m	0.005 m
Z	1000455.193 m	0.002 m
Latitude	09° 04' 53.52408" N	0.001 m
Longitude	38° 54' 24.05972" E	0.003 m
El. Height	2452.619 m	0.006 m

This study has used processing result from the recent epoch ITRF2008 at epoch 2016.96 because this result is to be compared with results obtained from other processing packages which are processed with recent epochs.

Table 4. 4: Geodetic coordinates as computed from RTX.

Station	Latitude in degree	Longitude in degree	Height(h) in meter	Standard deviation in meter		
				Latitude	Longitude	Height(h)
CCDG	9.072482858	38.89480113	2463.638	0.003	0.001	0.006
LIBA	9.081534467	38.90668326	2452.619	0.003	0.001	0.006
RSVR	9.053908994	38.87318469	2476.825	0.005	0.002	0.008
LDHC	9.09043475	38.91337636	2461.232	0.003	0.001	0.006
LESL	9.0646766	38.88412984	2453.421	0.004	0.001	0.006

4.1.4 Leica Geo Office (LGO)

Leica Geo Office software processes GNSS observation data in both rinex and m00 file format. Data from five local GNSS bench marks were processed with a tie to ADIS IGS station. The observation data at each station was observed for 72 hours. LGO is limited to process data at maximum of 1km processing baseline length (see, GPS-processing Parameters: Strategy, Fix ambiguities up to). In order get better result it is recommended to use more reference stations during processing. But, there are no other stable and continuously operating stations near to the study area other than ADIS. This is the reason why we used only ADIS station to process the data. The position and velocity solutions of the ADIS station was determined through adjustment to some local continuously operating stations (ABOO, ARMI, ASOS, ASAB, NAZR) and IGS stations used are (MBAR, MAL2, NKLG, SUTH, SUTM and ONSA) for time span of 2007 to 2015. The solutions of the reference ADIS station were determined using Gamit/Globk on the basis of daily, monthly and yearly time series providing geodetic quality coordinates 9.03513606 degree latitude, 38.76630439 degree longitude and 2439.146m ellipsoidal height (h). These values are used to adjust the local solutions at five GNSS-levelling bench marks (Figure 4.5, Table 4.6).

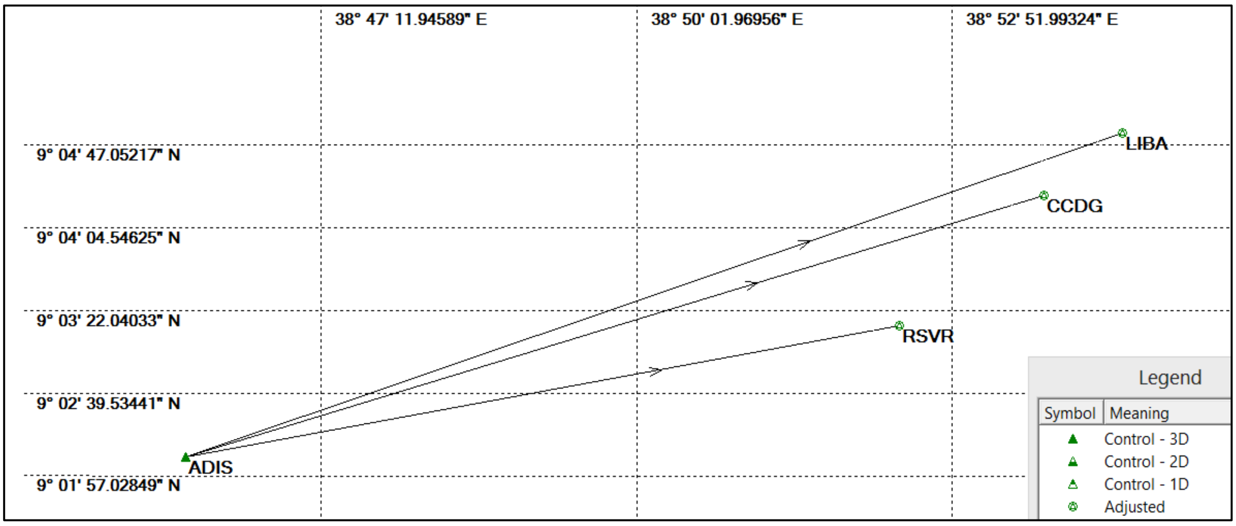

Figure 4. 5: Data processing scheme of LGO for doy350.

On top of computing stations coordinates, LGO is capable of plotting the residuals of code and phase for single, double and triple differences as well as DOP, elevation and azimuth for the computed coordinates (Figure 4.6).

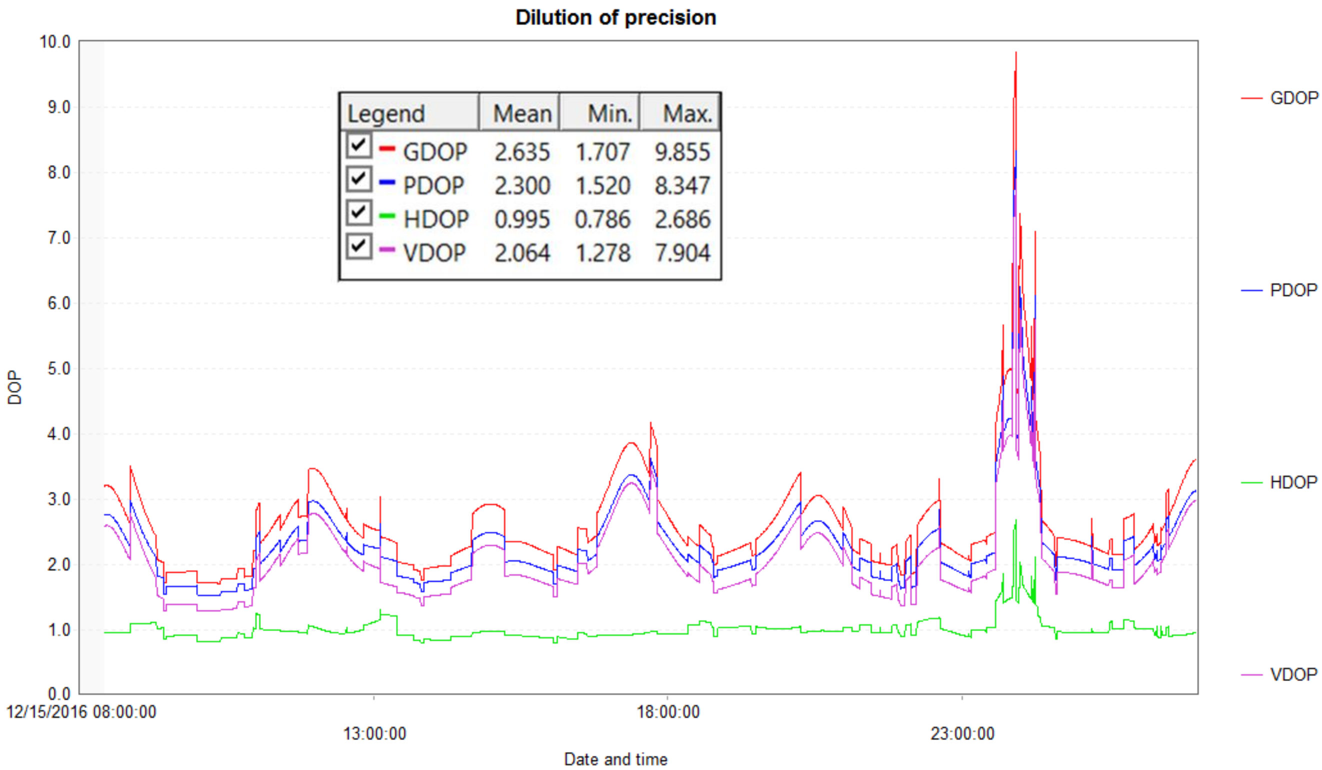

Figure 4. 6: Time series DOP values from LGO data processing.

Table 4. 5: Geodetic coordinates as computed from LGO.

Station	Latitude in degree	Longitude in degree	Height(h) in meter	Standard deviation in meter		
				Latitude	Longitude	Height(h)
CCDG	9.072482	38.8948	2463.578	0.002	0.001	0.004
LIBA	9.081534	38.90668	2452.621	0.002	0.002	0.005
RSVR	9.053908	38.87318	2476.721	0.001	0.001	0.003
LDHC	9.090434	38.91338	2461.25	0.002	0.001	0.004
LESL	9.064676	38.88413	2453.387	0.001	0.001	0.004

4.1.5 Error analysis

The position coordinates of the five bench marks are predicted with some magnitude of error depending on the nature of the processing method used. The standard error depends on the capability of the software packages and the parameters used while processing. The magnitude of error being small does not mean that the result predicted to that extent is better than results obtained from other processing methods. Rather, it indicates variance between the local solutions – a better accuracy assessment can be made by comparing it with other independent solutions. The magnitude of errors in east, north and height components are described in (Figures 4.7, 4.8 and 4.9) below.

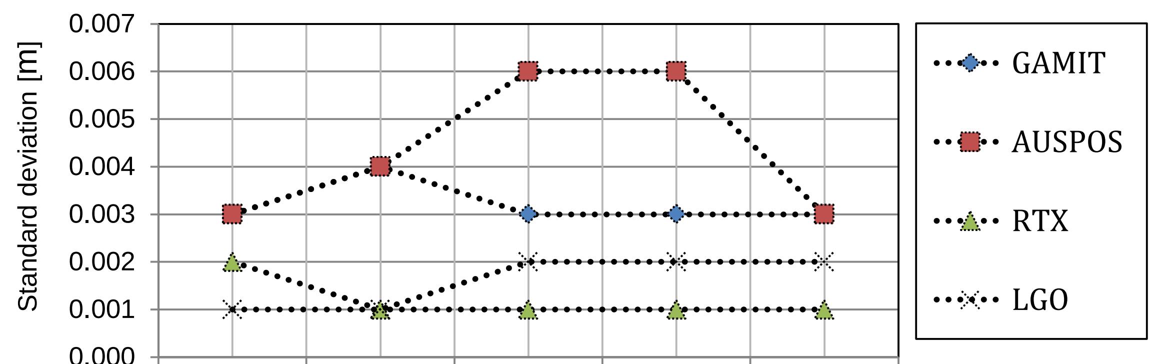

	RSVR	LESL	CCDG	LIBA	LDHC
GAMIT	0.003	0.004	0.0030	0.003	0.003
AUSPOS	0.003	0.004	0.006	0.006	0.003
RTX	0.002	0.001	0.001	0.001	0.001
LGO	0.001	0.001	0.002	0.002	0.002

Figure 4. 7: Magnitude of error in East component

Figure 4.7 shows the extent of errors for RTX and LGO are almost the same for bench marks RSVR, LESL and LDHC. For the same bench marks, the solutions are the identical for GAMIT and AUSPOS. Overall, the error in the east component ranges from 0.001m to 0.006m.

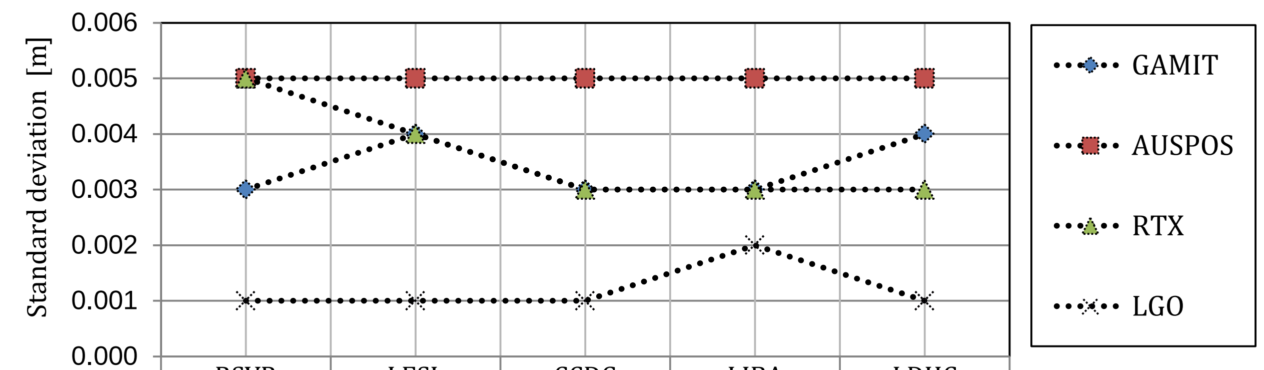

	RSVR	LESL	CCDG	LIBA	LDHC
GAMIT	0.003	0.004	0.003	0.003	0.004
AUSPOS	0.005	0.005	0.005	0.005	0.005
RTX	0.005	0.004	0.003	0.003	0.003
LGO	0.001	0.001	0.001	0.002	0.001

Figure 4. 8: Magnitude of error in North component

Based on figure 4.8, the extent of errors in GAMIT and RTX are nearly the same whereas for LGO it is relatively low. Totally the error ranges from 0.001m to 0.005m in the north component.

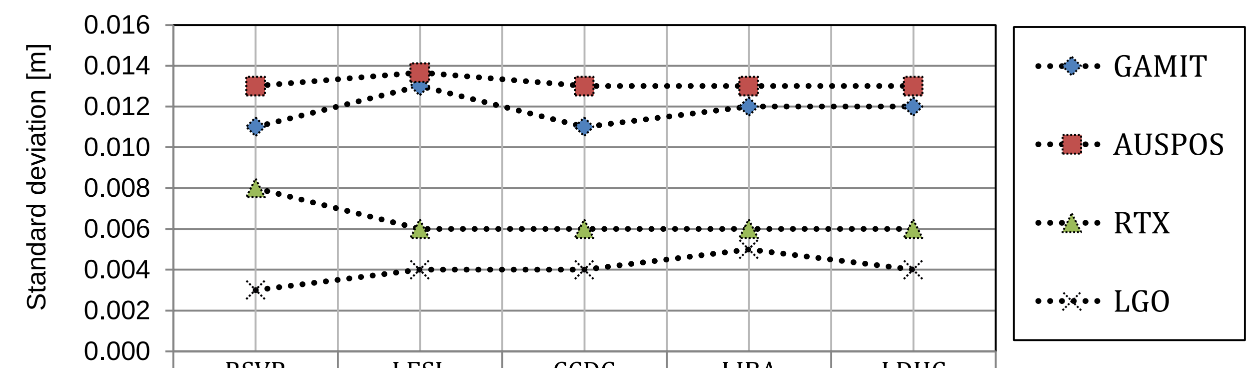

	RSVR	LESL	CCDG	LIBA	LDHC
GAMIT	0.011	0.013	0.011	0.012	0.012
AUSPOS	0.013	0.014	0.013	0.013	0.013
RTX	0.008	0.006	0.006	0.006	0.006
LGO	0.003	0.004	0.004	0.005	0.004

Figure 4. 9: Magnitude of error in height component.

Figure 4.9 illustrates that the error for GAMIT and AUSPOS is close to each other and the standard deviation for RTX and LGO are the same. For the height component, the error ranges from 0.003m to .014m. But, mostly the height component is predicted from GNSS observation approximately at about 1cm to 2cm level of standard deviation. Therefore, height predictions from GAMIT and AUSPOS are more likely promising if and only if good geometry of network adjustment baseline exists.

4.1.6 Accuracy assessment

GNSS data has been processed using different software packages and results obtained from each were presented in section 4.1. This study has computed the residuals in easting, northing and height, and Tables 4.7, 4.8 and 4.9 present the mean and standard deviation of the residuals. The scatter plots of the residuals are illustrated in Figures 4.10, 4.11 and 4.12.

Table 4. 6: Mean and standard deviation of residuals in East component

WGS 84 UTM ZONE 37 Easting [m]						
Station	Gamit	Auspos	RTX	LGO		
CCDG	488439.471	488439.482	488439.477	488439.358		
LIBA	489745.483	489745.493	489745.487	489745.373		
LESL	487266.495	487266.514	487266.511	487266.395		
LDHC	490481.209	490481.229	490481.223	490481.102		
RSVR	486063.272	486063.284	486063.283	486063.160		
Residuals [m]						
Station	Gamit minus Auspos	Gamit minus RTX	Gamit minus LGO	Auspos minus RTX	Auspos minus LGO	RTX minus LGO
CCDG	-0.011	-0.006	0.112	0.005	0.123	0.119
LIBA	-0.010	-0.004	0.111	0.006	0.121	0.115
LESL	-0.019	-0.015	0.100	0.004	0.119	0.115
LDHC	-0.020	-0.014	0.107	0.006	0.127	0.121
RSVR	-0.012	-0.011	0.111	0.001	0.123	0.122
Mean	-0.014	-0.010	0.108	0.004	0.123	0.118
Stdev.	0.005	0.005	0.005	0.002	0.003	0.003

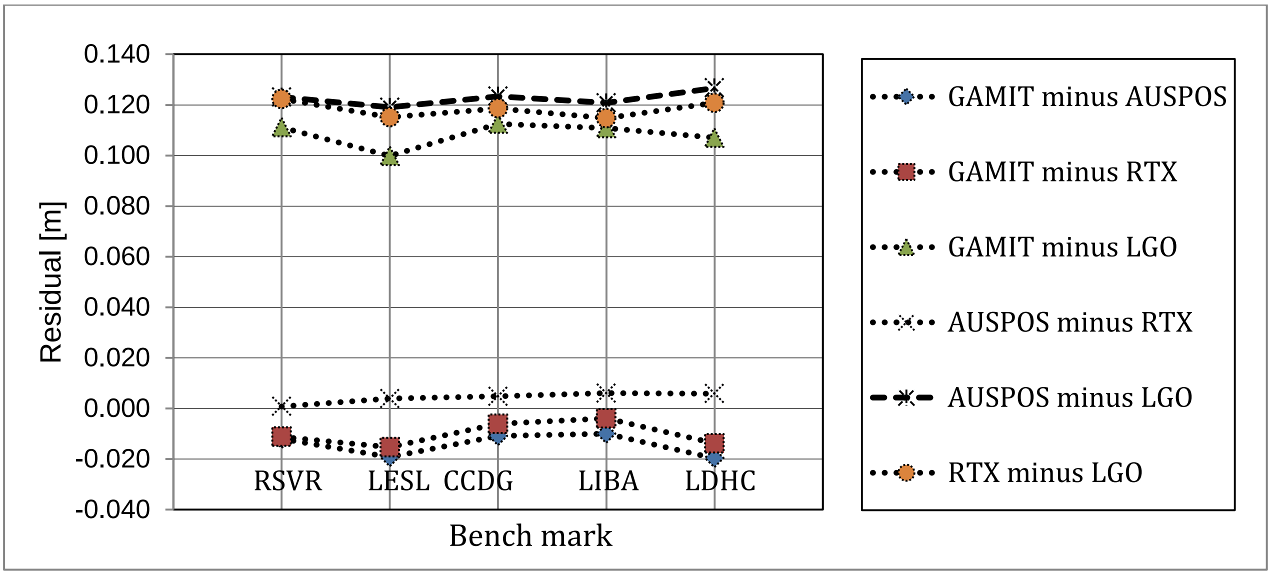

Figure 4. 10: Scatter of residuals across bench marks in East component

Table 4. 7: Mean and standard deviation of residuals in North component

WGS84 UTM Zone 37 Northing				
Station	Gamit	Auspos	RTX	LGO
CCDG	1002867.378	1002867.380	1002867.369	1002867.281
LIBA	1003867.749	1003867.750	1003867.739	1003867.647
LESL	1002004.688	1002004.694	1002004.683	1002004.599
LDHC	1004851.558	1004851.563	1004851.553	1004851.460
RSVR	1000814.649	1000814.652	1000814.641	1000814.553

Residuals [m]						
Station	Gamit minus Auspos	Gamit minus RTX	Gamit minus LGO	Auspos minus RTX	Auspos minus LGO	RTX minus LGO
CCDG	-0.002	0.009	0.097	0.011	0.099	0.088
LIBA	-0.001	0.010	0.101	0.011	0.103	0.092
LESL	-0.006	0.005	0.089	0.011	0.095	0.084
LDHC	-0.005	0.005	0.097	0.010	0.103	0.092
RSVR	-0.003	0.008	0.096	0.010	0.099	0.089
mean	-0.003	0.007	0.096	0.011	0.100	0.089
Stdev.	0.002	0.002	0.004	0.000	0.003	0.003

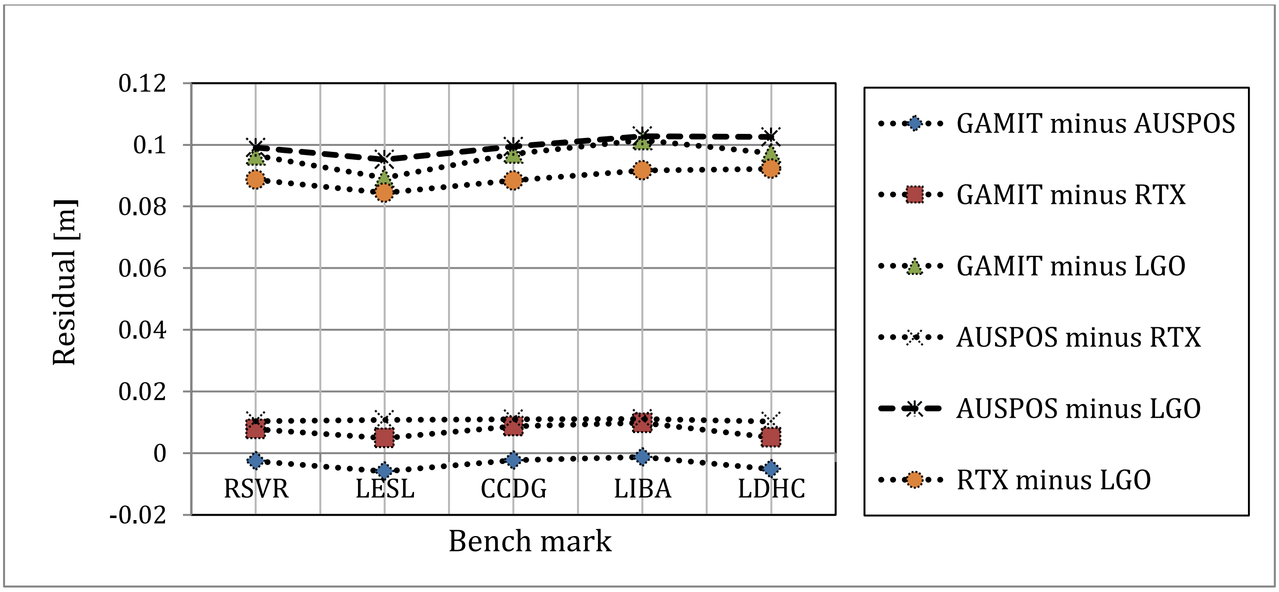

Figure 4. 11: Scatter of residuals across bench marks in North component

Table 4. 8: Mean and standard deviation of residuals in height component

Ellipsoidal Height[m]				
Station	Gamit	Auspos	RTX	LGO
CCDG	2463.615	2463.633	2463.638	2463.578
LIBA	2452.603	2452.620	2452.619	2452.621
LESL	2453.404	2453.476	2453.421	2453.387
LDHC	2461.219	2461.229	2461.232	2461.250
RSVR	2476.808	2476.829	2476.825	2476.721

Residuals[m]						
Station	Gamit minus Auspos	Gamit Minus RTX	Gamit Minus LGO	Auspos minus RTX	Auspos minus LGO	RTX Minus LGO
CCDG	-0.018	-0.023	0.037	-0.005	0.055	0.061
LIBA	-0.017	-0.016	-0.017	0.001	-0.001	-0.002
LESL	-0.071	-0.017	0.017	0.055	0.089	0.034
LDHC	-0.009	-0.012	-0.030	-0.003	-0.021	-0.018
RSVR	-0.020	-0.017	0.087	0.004	0.107	0.104
mean	0.018	0.003	0.035	0.018	0.046	0.037
Stdev.	0.025	0.004	0.047	0.025	0.056	0.049

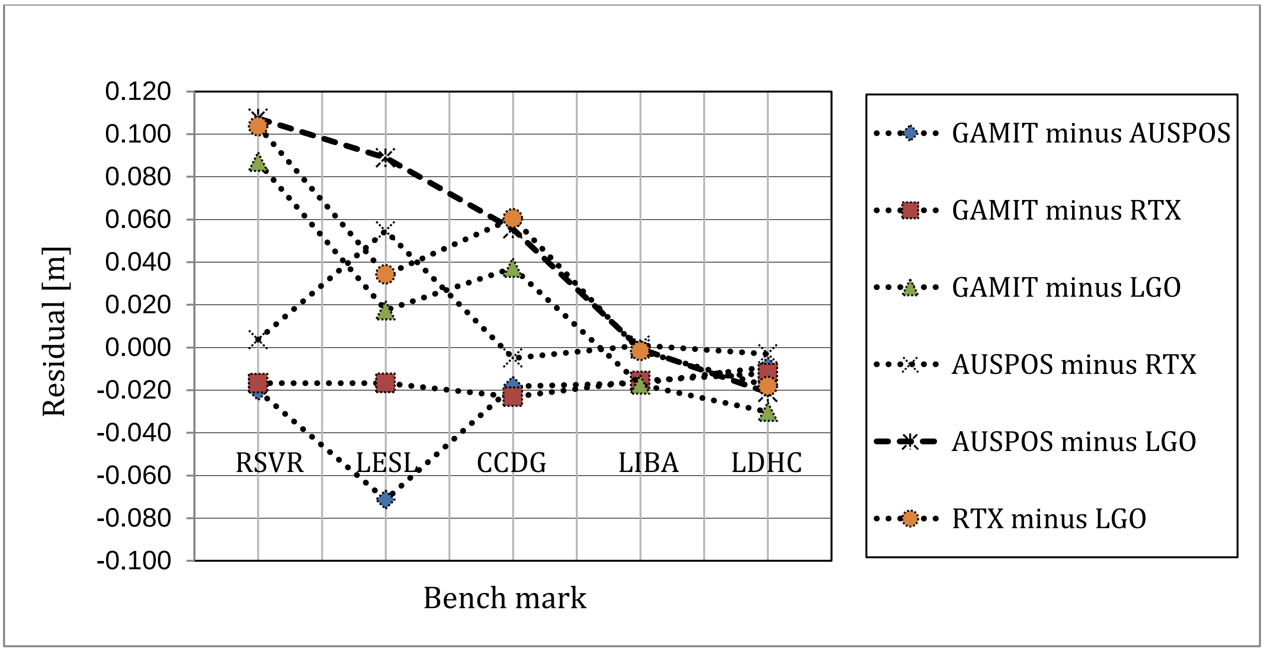

Figure 4. 12: Scatter of residual across bench marks in height component

From Figures 4.10 and 4.11 one can see that the residual between coordinates derived from Gamit/Globk, Auspos and RTX are small ranging from -0.02m to 0.02m. Whereas, the mismatch between LGO's coordinates and the corresponding coordinates derived from other software packages is relatively larger. The disagreement of coordinates derived from LGO with solutions estimated from other software packages is due to the fact that the processing of the data using LGO was only tied to ADIS reference station (section 4.1.4). Therefore, this could not make good network of processing baseline for the adjustment of GNSS/levelling bench marks to be used (See, Figure 4.5).

Besides, the residuals between AUSPOS, RTX and GAMIT are more likely small (Figures 4.10, 4.11 and 4.12). The noticeable difference between the solution of GAMIT compared to AUSPOS and RTX is due to the fact that the distribution of reference IGS stations are not even and the network is not the same. Most of the reference stations used by the online processing software packages/services are located nearby each other in northern and only one station (ZAMB) is located south of the local bench marks (Figure 4.4). At this stage it should be noted that the selection of the IGS stations are out off control of the users.

In contrast, Gamit/Globk uses IGS stations which are selected on the basis of making a good geometry with respect to local stations (see, Figure 4.1). This is to mean that the selected IGS stations are distributed so that the local stations are relatively at mid of these stations as the length of base line in network adjustment has a significant effect on the results of the processing.

In relation to this, Figure 4.12 shows that the solutions derived from LGO are in general deviating from the ones obtained from others. This mismatch is caused by poor baseline network of the LGO.

Therefore, this study has used the Gamit/Globk derived geodetic coordinates for computing geopotential heights from Earth Gravity Models using space domain spherical harmonic analysis. The results of this analysis will be presented in the next section.

4.2 Levelling Result

The study has determined precise levelling heights at five GNSS-levelling bench marks tied to nearby first order bench mark located along the main asphalt road covering total distance of 10.742 km base line (see, Figure 1.2). Levelled heights with misclosure are described in Table 4.10. For detail of descriptions of bench marks, readers are encouraged to see Annex C up to Annex G.

Table 4. 9: Precise levelled height

From bench mark	Through bench mark	To bench mark	Distance in meter	Misclosure in meter	GNSS-levelling bench mark	Levelled height (H_{Level}) in meter
KARALLO	TANK	KARALLO	4307.100	0.025		
TANK	KELA	TANK	2950.800	0.004		
TANK	RSVR	TANK	184.700	0.000	***RSVR***	***2482.846***
KELA	LESL	KELA	1342.400	0.004	***LESL***	***2459.456***
KELA	CCDG	KELA	4107.300	0.029	***CCDG***	***2469.761***
CCDG	LIBA	CCDG	3498.300	0.023	***LIBA***	***2458.823***
LIBA	KBL2 & TPPL	LIBA	4168.800	0.028		
TPPL	LDHC	TPPL	1108.300	0.004	***LDHC***	***2467.461***

4.3 Derived geopotential heights

Geopotential heights can be computed either by using Stokes like integral that uses gravity anomalies/disturbances or space-domain spherical harmonic analysis that uses a set of dimensionless cosine and sine coefficients of the global geopotential mode. This study has used Space-domain spherical harmonic analysis to compute geoid and geopotential heights directly from a set of dimensionless Stoke's cosine and sine coefficients. With the use of spherical harmonic analysis, geopotential heights are computed using equations 3.4 to 3.10 (for more information see chapter three).

The "Tg_Schmidt" and "Tg_Interp" FORTRAN programs are used for the computation of geopotential height from combined(GOCO03S and EGM08) and EIGEN-6C4 geopotential models. These programs were used to compute geoid or geopotential heights at each bench mark directly from coefficient of the combined model (GOCO03S and EGM2008) and EIGEN-6C4 global geopotential models at five GNSS/levelling bench marks located across the main asphalt road from Addis Ababa city to Legedadi town. The resulting geopotential heights from both models are compared with levelled heights (Tables 4.11 and Table 4.12).

Table 4. 10: Levelled heights compared with geopotential heights derived from GOCO03S and EGM08 model.

Station	Geopotential number(C) in m^2s^{-2}	Ellipsoidal height(h) in meter	H_{Levl} in meter	H_{ortho} In meter	H_{normal} in meter	h-N in meter	h-zeta in meter
CCDG	24149.658	2463.615	2469.761	2469.7044	2469.8436	2469.6752	2469.846
LIBA	24041.954	2452.603	2458.823	2458.6963	2458.8235	2458.6685	2458.826
RSVR	24279.026	2476.808	2482.846	2482.9377	2483.0808	2482.9081	2483.083
LDHC	24125.938	2461.219	2467.461	2467.292	2467.4154	2467.2646	2467.418
LESL	24049.936	2453.404	2459.456	2459.4961	2459.6413	2459.4659	2459.644

Height prediction

Station	H_{Level}-H_{Ortho}	H_{Level}-(h-N)	H_{Level}-(h-zeta)	H_{Level}-$H_{Helmert}$
CCDG	0.057	0.086	-0.085	1.470
LIBA	0.127	0.154	-0.003	1.508
RSVR	-0.092	-0.062	-0.237	1.313
LDHC	0.169	0.196	0.043	1.564
LESL	-0.040	-0.010	-0.188	1.334
mean	0.044	0.073	-0.094	1.438
Stdev.	0.110	0.109	0.119	0.110

Table 4. 11: Levelled heights compared with geopotential heights derived from EIGEN-6C4 model

Station	Geopotential number(C) in m^2s^{-2}	Ellipsoidal height(h) in meter	H_{Level} in meter	H_{Ortho} in meter	H_{normal} in meter	h-N in meter	h-zeta in meter
CCDG	24149.300	2463.615	2469.761	2469.669	2469.808	2469.639	2469.810
LIBA	24041.590	2452.603	2458.823	2458.658	2458.787	2458.63	2458.789
RSVR	24278.660	2476.808	2482.846	2482.899	2483.043	2482.869	2483.046
LDHC	24125.560	2461.219	2467.461	2467.251	2467.377	2467.223	2467.380
LESL	24049.580	2453.404	2459.456	2459.460	2459.605	2459.43	2459.608

Height prediction

Station	H_{Level}-H_{ortho}	H_{Level}-(h-N)	H_{Level}-(h-zeta)	H_{Level}-$H_{Helmert}$
CCDG	0.092	0.122	-0.049	1.507
LIBA	0.165	0.193	0.034	1.777
RSVR	-0.053	-0.023	-0.200	1.582
LDHC	0.210	0.238	0.081	1.835
LESL	-0.004	0.026	-0.151	1.601
mean	0.082	0.111	-0.057	1.660
Stdev.	0.111	0.110	0.119	0.139

4.4 Geopotential models evaluation

The accuracy of EIGEN-6C4, the combined geopotential model (GOCO03S and EGM08) and are evaluated by comparing them with GNSS-levelling data. The gravimetric geoid heights computed from both models are compared with the geoid obtained from GNSS-levelling. Besides the orthometric heights predicted from geopotential models are compared with levelled heights. The accuracy of the two geopotential models was also investigated by comparing different forms of gravity based heights with GNSS-levelling data.

4.4.1 Combined geopotential model (GOCO03S and EGM08) evaluation

Table 4.11 shows the misfit between the gravimetric geoid derived from the combined geopotential model (GOCO03S and EGM08) and geometric geoid determined from GNSS-levelling in terms of mean and standard deviation. The residuals between the orthometic heights determined directly from the combined geopotential model and levelled heights at five bench marks have a mean of 0.044m and standard deviation of 0.110m. The mean value represents the vertical distance separation (vertical offset/datum shift) between the geoid and the mean sea level to which the levelled heights are connected – levelled heights in Ethiopia are tied to historical tide gauge station located at the port of Alexander, Egypt.

Whereas, the standard deviation shows the accuracy of predicting orthometric height using the geopotential model as compared to levelled heights. The mean and standard deviation between the combined (GOCO03S and EGM08) model and levelling height was found to be -0.044m and 0.039m respectively from early independent experimental test performed by Waktola (2013) across 100km levelling route between Addis Ababa and Adama. The result of this study is in a good agreement with the accuracies reported by Waktola (2013); improvement has been achieved in the mean value with a little increase in the baise. Table 4.11 shows the comparison between different forms of heights. For instance, the difference between geoid derived from geopotential model and geoid obtained from GNSS-levelling has a mean of 0.073m and standard deviation of 0.109m. The mismatch between the GNSS-levelling and the gravimetric zeta heights has also a mean of -0.094m and standard deviation of 0.119m. The residuals between levelled heights and Helmert Orthometric heights have a mean of 1.438m and standard deviation of 0.110m. This indicates that the datum shift between levelled heights and Helmert orthometric heights has a large mean value of 1.438m. This might be due to the drawback of Helmert's assumption that the density variation of the subsurface is considered to be constant $\rho = 2.67g/cm^3$ throughout the earth. The comparison between levelled heights and orthometric heights is well presented in Figure 4.13. Table 4.13 illustrates correlation among different geopotential heights such as orthometric height

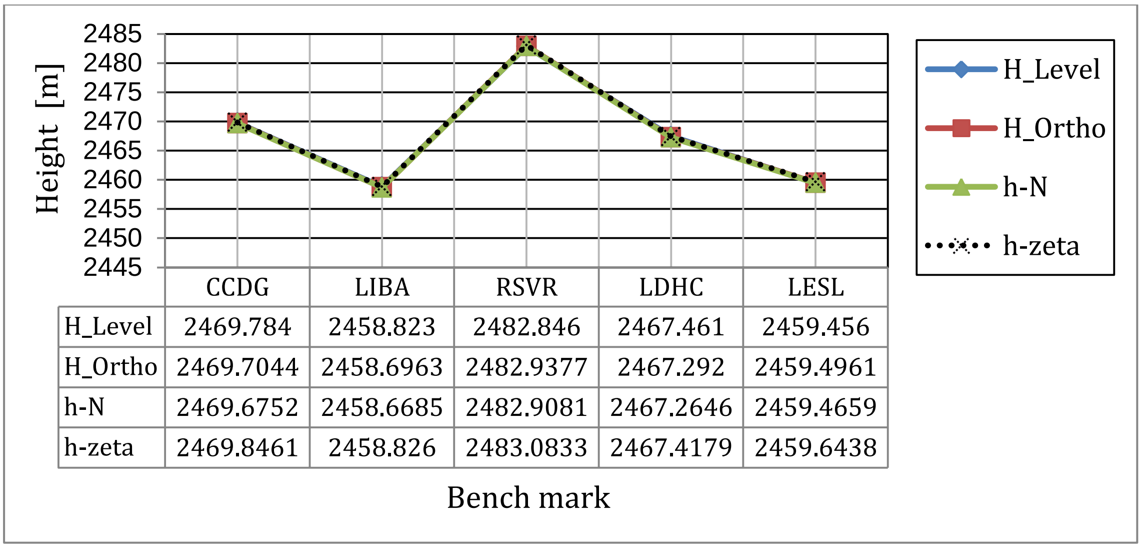

Figure 4. 13: Comparison of levelled height with orthometric heights derived from combined (GOCO03S and EGM08) geopotential model

Also, Figure 4.13 indicates strong relationship between different forms of orthometric heights that are evaluated at each GNSS-levelling bench mark.

Table 4. 12: Correlation of orthometric heights (i.e. levelled heights and orthometric heights estimated from the combined geopotential model)

Correlation	H_{Level}	H_{Ortho}	h-N	h-zeta
H_{Level}	1	0.999950543	0.99995161	0.999941625
H_{Ortho}	0.999950543	1	0.99999999	0.999999557
h-N	0.999951608	0.999999993	1	0.999999439
h-zeta	0.999941625	0.999999557	0.99999944	1

Correlation is statistical technique that can show whether and how strongly pairs of variables (data sets) are related. The correlation between data ranges from -1 to 1. Positive correlation exists where the high values of one data set are associated with high values of other data set. Negative correlation means association of high values of one with low values of other(s). Values close to 1 indicate a high degree of positive correlation, values close to -1 indicate a high degree of negative correlation and values of zero indicate no correlation at all. Table 4.13 shows that levelled heights and orthometric heights predicted from combined geopotential model has high degree of positive correlation.

4.4.2 EIGEN-6C4 geopotential model evaluation

The accuracy of the recently released EIGEN-6C4 geopotential was assessed using an independent GNSS-levelling data. Table 4.12 shows the mismatch between the gravimetric geoid based on the geopotential model and geometric geoid derived from GNSS-levelling data. Comparisons were also made between different types of geopotential heights and GNSS-levelling data. For five GNSS-levelling samples the difference between gravimetric orthometric heights and levelled heights has a mean of 0.082m and standard deviation of 0.111m. The misfit between gravimetric geoid and geoid calculated from GNSS-levelling have a mean of 0.111m and standard deviation of 0.110m. Whereas, the deviation between the geometric geoid (ellipsoidal height-levelled height) and EIGEN-6C4 based zeta heights has also a mean of -0.057m and standard deviation of 0.119m. The deviation between levelled heights and Helmert Orthometric heights is significant compared to residuals obtained by subtracting elevation values between pair of any two other height types accounting for a mean of 1.660m and standard deviation of 0.139m. The larger mean value between levelled height and Helmert orthometric height is due to Helmert's assumption that the density variation of the sub surface is considered to be constant.

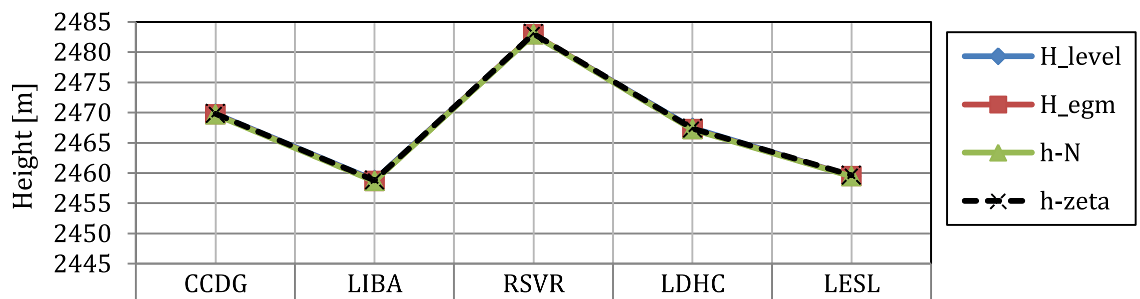

	CCDG	LIBA	RSVR	LDHC	LESL
H_level	2469.784	2458.823	2482.846	2467.461	2459.456
H_egm	2469.6686	2458.6578	2482.8991	2467.2507	2459.4602
h-N	2469.6392	2458.6296	2482.8692	2467.2227	2459.4299
h-zeta	2469.81	2458.7889	2483.0459	2467.3797	2459.6075

Bench mark

Figure 4. 14: Comparison of levelled height with orthometric heights derived from EIGEN-6C4 geopotential model.

Table 4. 13: Correlation of orthometric heights (i.e. Levelling, EIGEN-6C4 geopotential model)

Correlation	H_{Level}	H_{Ortho}	*h-N*	*h-zeta*
H_{Level}	1	0.9999	0.9999	0.9999
H_{Ortho}	0.9999	1	1	1
h-N	0.9999	1	1	1
h-zeta	0.9999	1	1	1

Table 4.14 shows high degree of correlation between levelled heights with other physical heights and among physical heights obtained from EIGEN-6C4 geopotential model. EIGEN-6C4 geopotential model has been evaluated in different parts of the world using GNSS-levelling data. Comparison of geoid heights determined point-wise by GNSS positioning and levelling is made with geoid heights derived from this geopotential model. Mean of GNSS-Levelling minus model-derived geoid heights are presented in table 4.15 below.

Table 4.14: GPS/Levelling fit in cm up to degree and order 2190.

[Source: 5th GOCE User Workshop, Paris, 25 – 28.11.2014]

Evaluation area	Number of bench marks	Root Mean Square (RMS) in cm
Europe	1234	20.9
Germany	675	4.8
Canada	1930	12.4
USA	6169	24.5
Australia	210	21.1
Japan	816	7.8
Brazil	672	30.6

In addition to GNSS-levelling validation approach, functions of gravity potential are also used for evaluation. Root mean square value of differences between EIGEN-6C4 and EGM2008 over the region of Ethiopia from spherically approximated gravity anomaly Δg and the second derivatives of the disturbing potential T_{zz} in radial direction have value of 4.4mGal and 1.3mGal respectively (Jaroslav Klokočník et a., 2015).

4.5 Comparison of EIGEN-6C4 and combined (GOGO03S and EGM08) geopotential model

These two models are evaluated independently using the same GNSS-levelling bench marks. The mean and standard deviation from the residual of levelled height and orthometric heights that are directly derived from the geopotential models are described in Table 4.11 and Table 4.12 for combined (GOGO03S and EGM08) and EIGEN-6C4 models, respectively.

From results of Table 4.11 and Table 4.12 one can see that the datum shift between the levelling height datum (mean sea level) and the geoid derived from the combined geopotential model is relatively better than geoid model/datum computed from EIGEN-6C4 model. Similarly, the accuracy of predicting orthometric height using combined geopotential model is better than the one derived from EIGEN-6C4 geopotential model. This may be due to the fact that EGM08 has incorporated local airborne gravity information over the region of Ethiopia containing medium to short wavelengths as well as the combined model has recovered long wavelengths to the highest accuracy from GOCO03S model. The combination algorithm that we employed, that is, the Butterworth filter may be clever enough than mathematical models use to synthesis Stoke's cosine and sine coefficients from surface gravity anomalies or gravity disturbances. On top of this, the EIGEN-6C4 model is in a good agreement with a mean of -0.038m and standard deviation of 0.002m to GOCO03S plus EGM08. The residuals between levelled height and orthometric height derived from both models are described in Figure 4.15 bellow.

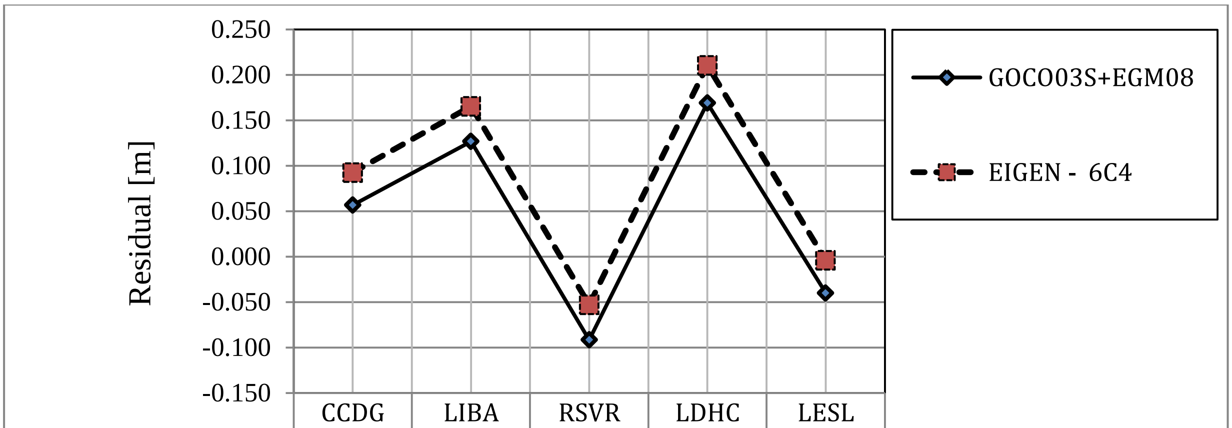

	CCDG	LIBA	RSVR	LDHC	LESL
GOCO03S+EGM08	0.057	0.127	-0.092	0.169	-0.040
EIGEN - 6C4	0.092	0.165	-0.053	0.210	-0.004

Figure 4. 15: Residuals between levelled height and orthometric height estimated from the combined (GOCO03S and EGM08) and EIGEN-6C4 geopotential models.

Chapter 5

5. Conclusions and Recommendations

5.1 Conclusions

The accuracy of the combined geopotential model (GOCO03S and EGM08) and EIGEN-6C4 geopotential model have been evaluated at five GNSS-levelling bench marks located along the main asphalt road between Addis Ababa City and Legedadi town. The results of the study shows that orthometric heights from the combined (GOCO03S and EGM08) and EIGEN-6C4 geopotential models are determined at an accuracy of 0.110m and 0.111m, respectively. The comparison made between the combined and EIGEN-6C4 geopotential shows both models are in a good agreement this may be due to the fact that both models incorporate long wavelength components of the gravity field from GOCE gravity satellite mission. There exist good correlation between levelled heights and orthometric heights derived from geopotential models.

5.2 Recommendations

- EIGEN-6C4 should be modified locally with detailed topographic data and higher resolution gravity data in regions where terrain is rougher without altering the long wavelength information so that it can simulate to levelled heights.
- As first order geodetic levelled heights are required for assessing the accuracy of geopotential models, the destroyed bench marks should be recovered and new levelling should be conducted to make the evaluation of the geopotential models in different parts of Ethiopia.
- The accuracy of the geopotential models must be adequately assessed over the entire region of Ethiopia before it will be used for operational application.
- The geopotential models must be updated with the release of new gravity models and gravity satellite missions.

Annexes

Annex A: IGS stations employed in Gamit/Globk Processing

IGS Station	Latitude in degree	Longitude in degree	Ellipsoidal height in meter	Standard deviation [m]		
				Lat.	Long.	height(h)
ADIS	9.035136899	38.76630555	2439.141	0.003	0.003	0.009
DRAG	31.59320287	35.39207307	31.834	0.002	0.005	0.012
MAL2	-2.996053536	40.19414556	-20.921	0.003	0.002	0.008
MOIU	0.288321359	35.2900115	2201.514	0.002	0.003	0.009
NKLG	0.353908606	9.672127337	31.505	0.002	0.002	0.009
NOT1	36.87584655	14.98978994	126.323	0.002	0.001	0.012
TEHN	35.69728423	51.33409605	1194.546	0.005	0.002	0.010
ZAMB	-0.353908606	28.31101422	1324.927	0.006	0.010	0.010

Annex B: KARALLO Geodetic vertical control bench mark description

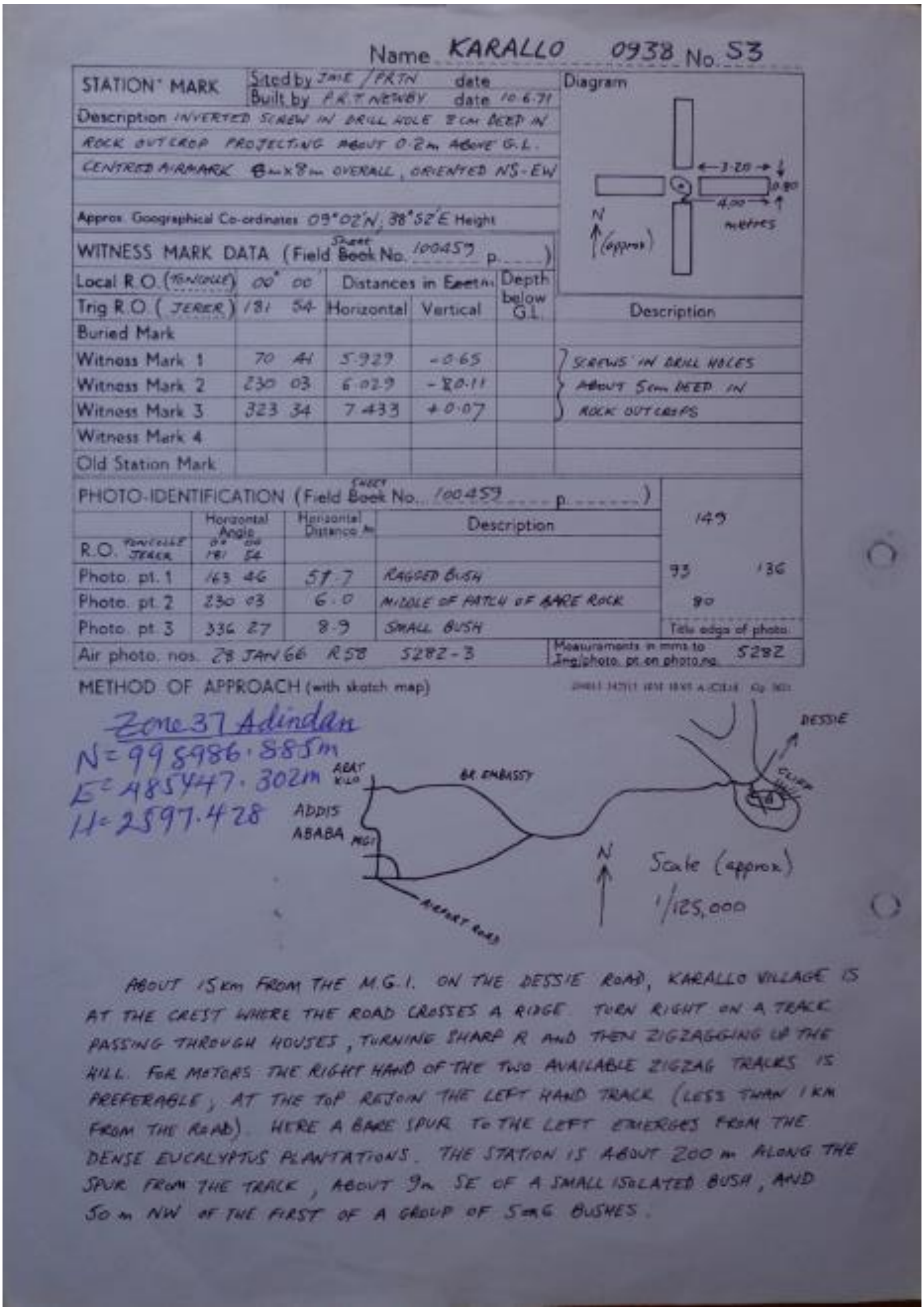

Name KARALLO 0938 No. 53

STATION MARK	Sited by JMIE / PRTN date	Built by P.R.T. NEWBY date 10.6.71

Description INVERTED SCREW IN DRILL HOLE 8 CM DEEP IN ROCK OUTCROP PROJECTING ABOUT 0.2m ABOVE G.L.
CENTRED AIRMARK 8m x 8m OVERALL, ORIENTED NS-EW

Approx. Geographical Co-ordinates 09°02'N, 38°52'E Height

Diagram

WITNESS MARK DATA (Field Sheet No. 100459 p. ....)

Local R.O. (TONICELLE) 00° 00'		Distances in metres: Horizontal	Vertical	Depth below G.L.	Description
Trig R.O. (JERER)	181 54				
Buried Mark					
Witness Mark 1	70 41	5.929	-0.65		SCREWS IN DRILL HOLES
Witness Mark 2	230 03	6.029	-80.11		ABOUT 5cm DEEP IN
Witness Mark 3	323 34	7.433	+0.07		ROCK OUTCROPS
Witness Mark 4					
Old Station Mark					

PHOTO-IDENTIFICATION (Field Sheet No. 100459 p. ......)

	Horizontal Angle	Horizontal Distance m	Description
R.O. TONICELLE / JERER	00 00 / 181 54		
Photo. pt. 1	163 46	57.7	RAGGED BUSH
Photo. pt. 2	230 03	6.0	MIDDLE OF PATCH OF BARE ROCK
Photo. pt. 3	336 27	8.9	SMALL BUSH

149
93 136
80
Title edge of photo

Air photo. nos. 28 JAN 66 R58 5282-3 — Measurements in mms to Ing/photo. pt on photo no. 5282

METHOD OF APPROACH (with sketch map)

Zone 37 Adindan
N=998986.885m
E=485447.302m
H=2597.428

ABOUT 15km FROM THE M.G.I. ON THE DESSIE ROAD, KARALLO VILLAGE IS AT THE CREST WHERE THE ROAD CROSSES A RIDGE. TURN RIGHT ON A TRACK PASSING THROUGH HOUSES, TURNING SHARP R AND THEN ZIGZAGGING UP THE HILL. FOR MOTORS THE RIGHT HAND OF THE TWO AVAILABLE ZIGZAG TRACKS IS PREFERABLE, AT THE TOP REJOIN THE LEFT HAND TRACK (LESS THAN 1 KM FROM THE ROAD). HERE A BARE SPUR TO THE LEFT EMERGES FROM THE DENSE EUCALYPTUS PLANTATIONS. THE STATION IS ABOUT 200 m ALONG THE SPUR FROM THE TRACK, ABOUT 9m SE OF A SMALL ISOLATED BUSH, AND 50 m NW OF THE FIRST OF A GROUP OF SMALL BUSHES.

Source: Ethiopian Mapping Agency (EMA)

Annex C: Bench mark RSVR description

Bench mark RSVR is established tied with bench mark TANK. TANK is tied with first order levelling bench mark KARALLO by conducting differential levelling for about 4307.1m from 107 turning points. Levelling was conducted on 21 8 2016 at the environmental temperature of 12 ^{0}c and partly sunny weather condition. The reduced Level of TANK from differential levelling is 2490.895m with misclosure of 0.025m. The levelled height of RSVR is **2482.846m** from 7 turning points, tied with TANK and established by conducting levelling for about 184m with the misclosure of 0.000m and established at location suitable for GNSS observation.

Station	Latitude in degree	Longitude in degree	Ellipsoidal Height in meter	Levelled height in meter	Tied with	Levelling distance	Miscl osure	Number of turning points
RSVR	9.053909065	38.87318459	2476.808	2482.846	TANK	184m	0.000	7

Annex D: Bench mark LESL description

Bench mark LESL is established tied with bench mark KELA. KELA is tied with bench mark TANK by conducting differential levelling for about 2950.8m from 65 turning points. The reduced Level of KELA from differential levelling is 2440.313m with misclosure of 0.004m. To establish LESL, Levelling was conducted on 19 12 2016 at the environmental temperature of 14 ^{0}c and partly sunny weather condition. The levelled height of LESL is **2459.456m,** tied with KELA and established by conducting levelling for about 1342.4m from 27 turning points with the misclosure of 0.004m. LESL is established at location suitable for GNSS observation.

Station	Latitude in degree	Longitude in degree	Ellipsoidal Height in meter	Levelled height in meter	Tied with	Levelling distance in meter	Miscl osure	Number of turning points
LESL	9.064676644	38.88412970	2453.404	2459.456	KELA	1342.4	0.004	27

Annex E: Bench mark CCDG description

Bench mark CCDG is established tied with bench mark KELA. Levelling was conducted on 22 8 2016 and 23 8 2016 at the environmental temperature of 17 ^{0}c and partly sunny weather condition. The levelled height of CCDG is **2469.761m**, tied with KELA and established by conducting levelling for about 4107.3m from 86 turning points with the misclosure of 0.029m. CCDG is established at location suitable for GNSS observation.

Station	Latitude in degree	Longitude in degree	Ellipsoidal Height (m)	Levelled height (m)	Tied with	Levelling distance (m)	Miscl osure (m)	Number of turning points
CCDG	9.072482937	38.89480107	2463.615	2469.761	KELA	4107.3	0.029	86

Annex F: Bench mark LIBA description

Bench mark LIBA is established tied with bench mark CCDG. To establish LIBA Levelling was conducted on 24 8 2016 at the environmental temperature of 12 ^{0}c and partly sunny weather condition. The levelled height of LIBA is **2458.823m,** tied with CCDG and established by conducting levelling for about 3498.3m from 73 turning points with the misclosure of 0.023m. CCDG is established at location suitable for GNSS observation.

Station	Latitude in degree	Longitude in degree	Ellipsoidal Height (m)	Levelled height (m)	Tied with	Levelling distance (m)	Miscl osure (m)	Number of turning points
LIBA	9.081534555	38.90668322	2452.603	2458.823	CCDG	3498.3	0.023	73

Annex G: Bench mark LDHC description

Bench mark LDHC is established tied with bench mark TPPL. Bench mark TPPL (63^{rd} turning point) was established during levelling work carried out on 24 08 2016 to tie LIBA with bench mark KBL2 (59^{th} turning point).

To establish KBL2 Levelling was conducted on 25 8 2016 at the environmental temperature of 7 ^{0}c and partly sunny weather condition. The levelled height of KBL2 from differential levelling is 2454.273m, tied with LIBA and established by conducting levelling for about 4168.8m from 92 turning points with the misclosure of 0.028m. The levelled height of TPPL is 2459.242m on this levelling line. LDHC is established at location suitable for GNSS observation. To establish bench mark LDHC levelling was conducted on 20 12 2016 at the environmental temperature of 14 ^{0}c and partly sunny weather condition. The levelled height of LDHC is **2467.461m**, tied with TPPL and established by conducting levelling for about 1108.3m from 25 turning points with the misclosure of 0.004m. CCDG is established at location suitable for GNSS observation.

Station	Latitude in degree	Longitude in degree	Ellipsoidal Height (m)	Levelled height (m)	Tied with	Levelling distance (m)	Miscl osure (m)	Number of turning points
LDHC	9.090434796	38.91337623	2461.219	2467.461	TPPL	1108.3	0.004	25

References

Andersen O.B (2010). The DTU10 Gravity field and Mean sea surface. Second International Symposium of the Gravity Field Service – IGFS2 20–22 September 2010, Fairbanks, Alaska.

Andersen O.B, Knudsen P. (2009). DNSC08 mean sea surface and mean dynamic topography model. Journal of Geophysical Research, 114(C11)

Barry F., Glenn B. (2000)). Surveying principle and application. 5th edition, United States of America.

Bedada T. (2010). An Absolute Geopotential Height System for Ethiopia. University of Edinburgh, Geosciences, School of Geography and the Lived Environment Research Institute Geography PhD thesis collection.

Blackwell H. (1962). The adjustment of Blue Nile vertical geodetic control project. Jornal of Geophysical Research, 67(11), 4421-4426, doi:1029/JZ067i011p04421.

Bruinsma S.L., F. C.-M.-C. (2014). ESA's satellite-only gravity field model via the direct approach based on all GOCE data. Geophysical Research Letters, 41(21), 7508–7514. doi:10.1002/2014gl062045.

Bursa M., K.R (1997). Determination of the geopotential scale factor from TOPEX/Poseidon satellite altimetry. Studia geoph. et geod., 41, 203-216.

Chandra A.M. (2005). Surveying: problem solving with theory and objective type questions. New Age International (p) limited, publishers, New Delhi.

Chen X., A. T. (2011). Trimble RTX, an innovative new approach for Network RTK. Proc. ION GNSS 2011, Portland, Oregon, 19-23 September.

Charles D. Ghilani, P. R. (2012). Elementary Surveying. An introduction to Geomatics. Thirteenth edition , India.

Ethiopia Geodetic survey (1957-1961). Ethiopia Geodetic survey report on horizontal and vertical surveys of the Blue Nile River basin by U.S. Department of commerce coast and Geodetic survey for Ethiopia-United states Cooperative Program for Water Resource.

Featherstone W.E., K. M. (2006). Height Systems and Vertical Datums: a Review in the Australian Context. Journal of Spatial Science, 51(1):21-42.

Förste C., S. L.-M.-J. (2014). EIGEN-6C4 The latest combined global gravity field model including GOCE data up to degree and order 2190 of GFZ Potsdam and GRGS Toulouse. 5th GOCE User Workshop, Paris, 25 – 28.11.2014.

Förste C. (2014). The latest combined global gravity field model including GOCE data up to degree and order 2190 of GFZ Potsdam and GRGS Toulouse. URL: http://icgem.gfz-potsdam.de/ICGEM/documents/Foerste-et-al-EIGEN-6C4.pdf.

Grafarend E. (1994). What is a geoid? In: Geoid and its Geophysical Interpretation. P.Vanicek and N.T. Christou (eds.), pp.1-32, CRC Press, Boca Raton.

Guochang Xu. (2007). GPS -Theory, Algorithm and Application. Second edition, Germany.

Heiskanen W. A. , Moritz H.(1967). Physical Geodesy. W. H. Freeman and Company; San Francisco, California and London, UK.

Hipkin RG. (2002). Defining the geoid by W = W_0= U_0: Theory and practice of a modern height system, in 'Gravity and Geoid 2002, 3rd Meeting of the International Gravity and Geoids Commission', Thessaloniki, Greece, 367-377.

Hofmann B., Moritz H. (2005). Physical Geodesy. Institute for Navigation and Satellite geodesy Technique, University Graz, Graz, Austria.

Jaroslav Klokočník, B. B. (2015). Evaluation of the gravity field modelEIGEN-6C4 in comparison with EGM2008by means of various functions of the gravity potential and by GNSS/levelling. Geoinformatics FCE CTU 14(1).

Jekeli C. (2000). Heights,the Geopotential and Vertical Datum's. Departement of Geodetic Science and Surveying, Report No.459, The Ohio State University, Columbus, USA.

Kebie B. (2013). Validation of the 2008 Earth Gravity Model using GPS and Levelling data : A case study in Addis Ababa and western part of Ethiopia. Civil engineering department under Geodesy , Addis Ababa University, Ethiopia.

Kiliçoğlu A., Direnç A., Simav M., Lenk O., Aktuğ B. and Yildiz H.(2008). Evaluation of the EGM2008 gravity model. In External Quality Evaluation Reports of EGM2008, Newton's Bull.4, Int. Assoc. of Geod. and the Int. Gravity Field Serv., Toulouse, France.

Kotsakis C., Katsambalos K., Ampatzidis D., Gianniou M. (2008). Evaluation of EGM2008 in Greece using GPS and levelling heights. IAG International Symposium on Gravity, Geoid and Earth Observation, Chania, Greece.

Metzler B., P. R.(2005). GOCE Data Processing: The Spherical Cap Regularization Approach. Studia Geophysica et Geodaetica, 49(4), 441–462, doi:10.1007/s11200-005-0021-5.

Mayer-Gürr T. (2007). ITG-Grace03s: The latest GRACE gravity field solution. Computed in Bonn; presented at the Joint International GSTM and SPP Symposium, Potsdam, Germany, 15–17 October.

Mayer-Gürr T., Rieser D., Hoeck E., Brockmann J.M., Schuh W.D., Krasbutter I.,Kusche J., Maier A.,Krauss S., Hausleitner W., Baur O., Jäggi A.,Meyer U., Prange L., Pail R., Fecher T., Gruber Th. (2012). The new combined satellite only model GOCO03S. International Symposium on Gravity, Geoid and Height Systems GGHS 2012, Venice, 10.10.2012.

Molodensky M., Eremeev V. and Yurkina M. (1962). Methods for study of external gravitational field and figure of the Earth. Jerusalem,Israel Program for Scientific Translations; [available from the Office of Technical Services, U.S. Dept. of Commerce, Washington], -1.

Moritz H. (1980). Advanced Physical Geodesy. Herbert Wichmann, Karlsruhe, Germany.

Moritz H. (1992). Geodetic Reference System 1980. Bulletin Géodésique, 66(2), 187-192.

Pail R., Bruinsma, S. Migliaccio F. Foerste C. , Goiginger H., Schuh W.-D. ,Hoeck E., Reguzzoni M., Brockmann J.M, Abrikosov O., Veicherts M., Fecher T., Mayrhofer R., Krasbutter I., Sanso F., Tscherning C.C. (2011). First GOCE gravity field models derived by three different approaches. Journal of Geodesy, 85, 11: 819-843.

Pavlis N.K, Holmes SA, Kenyon SC and Factor JK. (2008). An Earth Gravitational Model to Degree 2160: EGM2008. General Assembly of the European Geosciences Union. Vienna, Austria.

Schwarz K.P, Sidris M.G., Forsberg R. (1980). Orthometric height without levelling. J.Surv.Engrg., ASCE, 113(1), 28-40.

Shako R., Förste C., Abrykosov O., Bruinsma S., MartyJ.-C., L emoine J.-M., Flechtner F., Neumayer K.-H., Dahle C. (2014). EIGEN-6C: A High-Resolution Global Gravity Combination Model Including GOCE Data - In: Flechtner F., Sneeuw N., Schuh W.-D. (Eds.), Observation of the System Earth from Space - CHAMP, GRACE, GOCE and future missions, (GEOTECHNOLOGIENScience ReportNo.20; Advanced Technologies in Earth Sciences), Berlin [u.a.]: Springer, 155-161.DOI 10.1007/978-3-642-32135-1_20, Print ISBN 978-3-642-32134-4 Online ISBN 978-3-642-32135-1.

Sjöberg, L.E. (1999). The IAG approach to the atmospheric geoid correction in Stokes' formula and a new strategy. Journal of Geodesy, 73(7), 362-366.

Teschering C.C. (1983). The role of high degree spherical harmonic expansions in solving geodetic problems. proc.Int.Ass.Geodesy (IAG) symp., vol.1, Department of Geodetic Science, The Ohio state university, Columbus, Ohio.

Waktola B. (2013). Hybrid model of GOCO03S satellite only and EGM2008: validation in case study of Hageremariam to Yabelo. Civil engineering department under Geodesy, Addis Ababa University, Ethiopia.

Worku E. (2013). Validation of the 2008 earth gravity model : A case study around Debre Birhan using independent GPS/levelling data. Civil engineering department under Geodesy, Addis Ababa University, Ethiopia.

W.Schfield , M.Breach(2007). Surveying engineering. Sixth edition ,Published by Elsevier Ltd ,UK.